



UNIVERSIDAD DE INVESTIGACIÓN DE TECNOLOGÍA EXPERIMENTAL YACHAY

Escuela de Ciencias Químicas e Ingeniería

Título: Biocompatible Thermo-Responsive poly(VCL-co-PEGDA) Hydrogels for Controlled Drug Delivery Systems

Trabajo de integración curricular presentado como requisito para
la obtención del título de Química

Autora

Romero Herdoiza Jocelyn Fernanda

Tutor

Ph.D Díaz-Barrios Antonio

Co-tutora

Ph.D González Gemma

Urcuquí, marzo del 2020

Urququí, 12 de marzo de 2020

SECRETARÍA GENERAL
(Vicerrectorado Académico/Cancillería)
ESCUELA DE CIENCIAS QUÍMICAS E INGENIERÍA
CARRERA DE QUÍMICA
ACTA DE DEFENSA No. UITEY-CHE-2020-00010-AD

En la ciudad de San Miguel de Urququí, Provincia de Imbabura, a los 12 días del mes de marzo de 2020, a las 12:30 horas, en el Aula CHA-02 de la Universidad de Investigación de Tecnología Experimental Yachay y ante el Tribunal Calificador, integrado por los docentes:

<u>Presidente Tribunal de Defensa</u>	Dra. LOPEZ GONZALEZ, FLORALBA AGGENY , Ph.D.
<u>Miembro No Tutor</u>	Dr. SAUCEDO VAZQUEZ, JUAN PABLO , Ph.D.
<u>Tutor</u>	Dr. DÍAZ BARRIOS, ANTONIO , Ph.D.

Se presenta el(la) señor(ita) estudiante **ROMERO HERDOIZA, JOCELYN FERNANDA**, con cédula de identidad No. **0704619899**, de la **ESCUELA DE CIENCIAS QUÍMICAS E INGENIERÍA**, de la Carrera de **QUÍMICA**, aprobada por el Consejo de Educación Superior (CES), mediante Resolución **RPC-SO-39-No.456-2014**, con el objeto de rendir la sustentación de su trabajo de titulación denominado: **Biocompatible Thermo-Responsive poly(VCL-co-PEGDA) Hydrogels for Controlled Drug Delivery Systems**, previa a la obtención del título de **QUÍMICO/A**.

El citado trabajo de titulación, fue debidamente aprobado por el(los) docente(s):

<u>Tutor</u>	Dr. DÍAZ BARRIOS, ANTONIO , Ph.D.
<u>Co - Tutor</u>	Dra. GONZALEZ VASQUEZ, GEMA , Ph.D.

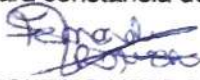
Y recibió las observaciones de los otros miembros del Tribunal Calificador, las mismas que han sido incorporadas por el(la) estudiante.

Previamente cumplidos los requisitos legales y reglamentarios, el trabajo de titulación fue sustentado por el(la) estudiante y examinado por los miembros del Tribunal Calificador. Escuchada la sustentación del trabajo de titulación, que integró la exposición de el(la) estudiante sobre el contenido de la misma y las preguntas formuladas por los miembros del Tribunal, se califica la sustentación del trabajo de titulación con las siguientes calificaciones:

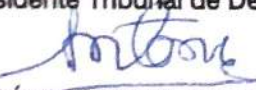
Tipo	Docente	Calificación
Tutor	Dr. DÍAZ BARRIOS, ANTONIO , Ph.D.	10,0
Miembro Tribunal De Defensa	Dr. SAUCEDO VAZQUEZ, JUAN PABLO , Ph.D.	9,9
Presidente Tribunal De Defensa	Dra. LOPEZ GONZALEZ, FLORALBA AGGENY , Ph.D.	9,8

Lo que da un promedio de: **9.9 (Nueve punto Nueve)**, sobre 10 (diez), equivalente a: **APROBADO**

Para constancia de lo actuado, firman los miembros del Tribunal Calificador, el/la estudiante y el/la secretario ad-hoc.


ROMERO HERDOIZA, JOCELYN FERNANDA
Estudiante



Dra. LOPEZ GONZALEZ, FLORALBA AGGENY , Ph.D.
Presidente Tribunal de Defensa


Dr. DÍAZ BARRIOS, ANTONIO , Ph.D.
Tutor





Dr. SAUCEDO VAZQUEZ, JUAN PABLO, Ph.D.
Miembro No-Tutor



ESCOBAR LANDAZURI, ANA MARIA
Secretario Ad-hoc

SECRETARÍA GENERAL
YACHAY TECH
ESCUELA DE INGENIERÍA QUÍMICA
CAMPUS QUÍMICA
ACTA DE DEFENSA DE TESIS DE GRADUACIÓN

Presidente del Jurado de Defensa: DR. DIEZ BARRIOS ANTONIO, Ph.D.
Miembro No-Tutor: DR. SAUCEDO VAZQUEZ JUAN PABLO, Ph.D.
Tutor: DR. DIEZ BARRIOS ANTONIO, Ph.D.

Se declara que el presente es un acta de la defensa de tesis de grado de la carrera de INGENIERÍA QUÍMICA, en el marco de la Ley de Educación Superior (L.E.S.) y el Reglamento de la L.E.S. emitido por el Ministerio de Educación Superior, Ciencia y Tecnología (M.E.S.C.T.) y el Consejo Superior de la Universidad Yachay Tech.

El presente acta de defensa de tesis de grado fue elaborado por el jurado de defensa de tesis de grado, integrado por el tutor y los miembros del jurado de defensa de tesis de grado, quienes han leído y discutido el contenido de la tesis de grado y han emitido su veredicto final.

Y por las declaraciones de los dos miembros del Jurado Calificador, las mismas son las siguientes:


Primero, aprobada la tesis de grado y recomendada el título de INGENIERO QUÍMICO, con una calificación de 8.8 (ocho punto nueve), sobre 10 (diez), equivalente a: APROBADO.

Tipo	Nombre	Calificación
Tutor	DR. DIEZ BARRIOS ANTONIO, Ph.D.	10.0
Miembro Titular de Defensa	DR. SAUCEDO VAZQUEZ JUAN PABLO, Ph.D.	8.8
Miembro Titular de Defensa	DR. LÓPEZ GONZÁLEZ FURBALBA ALEJY, Ph.D.	8.8


Lo que da lugar a la presente de 8.8 (ocho punto nueve), sobre 10 (diez), equivalente a: APROBADO.

Para constancia de lo actuado, firmen los miembros del Jurado Calificador, el/la estudiante y el/la secretario/a.




ROMÁN BDOIZA JOCELYN FERNANDA
Estudiante


DR. LÓPEZ GONZÁLEZ FURBALBA ALEJY, Ph.D.
Presidente Titular de Defensa


DR. DIEZ BARRIOS ANTONIO, Ph.D.
Tutor

AUTORÍA

Yo, **JOCELYN FERNANDA ROMERO HERDOIZA**, con cédula de identidad 0704619899, declaro que las ideas, juicios, valoraciones, interpretaciones, consultas bibliográficas, definiciones y conceptualizaciones expuestas en el presente trabajo; así cómo, los procedimientos y herramientas utilizadas en la investigación, son de absoluta responsabilidad de el/la autor(a) del trabajo de integración curricular. Así mismo, me acojo a los reglamentos internos de la Universidad de Investigación de Tecnología Experimental Yachay.

Urcuquí, marzo 2020.



Jocelyn Fernanda Romero Herdoiza

CI: 0704619899

AUTORIZACIÓN DE PUBLICACIÓN

Yo, **JOCELYN FERNANDA ROMERO HERDOIZA**, con cédula de identidad 0704619899, cedo a la Universidad de Tecnología Experimental Yachay, los derechos de publicación de la presente obra, sin que deba haber un reconocimiento económico por este concepto. Declaro además que el texto del presente trabajo de titulación no podrá ser cedido a ninguna empresa editorial para su publicación u otros fines, sin contar previamente con la autorización escrita de la Universidad.

Asimismo, autorizo a la Universidad que realice la digitalización y publicación de este trabajo de integración curricular en el repositorio virtual, de conformidad a lo dispuesto en el Art. 144 de la Ley Orgánica de Educación Superior

Urcuquí, marzo 2020.



Jocelyn Fernanda Romero Herdoiza
CI: 0704619899

This page is intentionally left blank.

TO MY PARENTS

*Juan Romero & Yolanda Herdoiza
for always loving and supporting me*

Acknowledgements

*“Don’t let the sun go down without saying thank you to someone,
and without admitting to yourself that absolutely no one gets this far alone.”*

Stephen King

I would like to take this opportunity to thank my academic advisors, Antonio Díaz, and Gemma González, for their guidance, encouragement, and useful critiques of this research work. I would also like to thank Hortensia Rodríguez, Flor Alba López, Ruth Oropeza, Lola de Lima, Thibault Terencio, and Kamil Makowski, for their advice and support in making this research possible. I would also like to extend my thanks to the technicians of the laboratory of the Escuela Politécnica Nacional for their help in doing the particle size measurements. My thanks are also extended to the School of Chemical Sciences and Engineering for giving me all the knowledge and skills to successfully develop this research work. I am very proud to have trained at Yachay Tech; I will always think that study here was my best decision.

My deep and sincere gratitude to my lovely family, my parents, Yolanda Herdoiza & Juan Romero, my brother, Darío Nivicela, my sisters, Diana Nivicela, Cristina Nivicela, & Maylin Romero, my nieces, Eliza Bush & Evolet Tinoco, and my nephews, Lucas Bush & Eduardo Nivicela, for their continuous and unparalleled love, help, support and encouragement throughout my career and my life. A special acknowledgment goes to my sister Maylin Romero who is my life partner and for always being there for me. Her support was undoubtedly important to reach this goal. Thank you all for believe in me and want the best for me.

At the end, I would like to express my greatest appreciation to all my friends who have helped and supported me throughout these five years at Yachay Tech. They are my second family. Thank you for motivated me every moment.

Fer Romero

Resumen

El tratamiento de varias enfermedades requiere medicamentos comúnmente administrados por vía oral o intravenosa. Dicha administración tiene varios inconvenientes, como el bajo control de los niveles de fármaco necesarios en plasma, lo que hace que el tratamiento sea ineficaz y, además, tenga efectos secundarios y baja compatibilidad con el paciente.[1]

Recientemente, el uso de hidrogeles sensibles a estímulos en sistemas controlados de administración de fármacos (DDS) se ha considerado una excelente alternativa debido a su biocompatibilidad inherente, su capacidad de respuesta a los cambios fisiológicos en el cuerpo y la diversidad de opciones de materiales tanto naturales como sintéticos.[2, 3]

El presente trabajo se centra principalmente en la síntesis, caracterización y capacidad de liberación de fármacos de los polímeros de poli(N-vinil caprolactama-co-poli (etilenglicol diacrilato)) poli(VCL-co-PEGDA), que muestran una respuesta de estímulo a la temperatura cercana a la temperatura fisiológica del cuerpo humano. Por esa razón, los cambios en el diámetro promedio de partícula hidrodinámica a diferentes temperaturas se estiman y se correlacionan con la velocidad de liberación del fármaco. El fármaco modelo elegido para los estudios de liberación es la colchicina, un fármaco potencial para el tratamiento de la enfermedad de gota, actualmente en desuso debido a su bajo índice terapéutico.[4]

La síntesis de cuatro hidrogeles de VCL-co-PEGDA que varían la concentración de reticulante de PEGDA se realizó con éxito por polimerización en emulsión. Su caracterización se realizó mediante espectroscopía DLS y FTIR. Los rendimientos de polimerización se estimaron mediante análisis de sólidos totales, y el *cloud point* de cada polímero se determinaron por UV-vis. Finalmente, el encapsulamiento y la liberación del fármaco a lo largo del tiempo se monitorizaron por HPLC y espectroscopía UV-vis que mostró que los perfiles de liberación del fármaco obtenidos corresponden a un sistema de suministro sostenido del fármaco.

Palabras clave: polímeros termosensibles, temperatura crítica inferior de la solución (LCST), nanogeles, sistemas de liberación de fármacos, colchicina.

Abstract

The treatment of several diseases requires drugs commonly administered orally or intravenously. Said administration has several drawbacks, such as low control of the necessary drug levels in plasma, which makes the treatment ineffective and in addition side effects and low compatibility with the patient.[1]

Recently, the use of stimuli-responsive hydrogels in controlled Drug Delivery Systems (DDSs) has been considered an excellent alternative because of its inherent biocompatibility, responsiveness to physiological changes in the body, and diversity of both natural and synthetic material options.[2, 3]

The present work focuses mainly on the synthesis, characterization, and drug release capacity of poly(N-vinyl caprolactam-co-poly(ethylene glycol) diacrylate)) poly(VCL-co-PEGDA) polymers, which show temperature stimuli-responsiveness near the physiological temperature of the human body. For that reason, the changes in the average hydrodynamic particle diameter at different temperatures are estimated and correlated with the drug release rate. The model drug chosen for releasing studies is colchicine, a potential drug for gout disease treatment, currently in disuse because of its low therapeutic index.[4] The synthesis of four VCL-co-PEGDA hydrogels varying the PEGDA crosslinker concentration was successfully carried out by emulsion polymerization. Their characterization was performed by DLS and FTIR spectroscopy. Polymerization yields were estimated by total solids analysis, and the cloud points were determined by UV-vis. Finally, the drug loading and release over time were monitored by HPLC and UV-vis spectroscopy showing that drug release profiles obtained corresponded to a sustained drug delivery system.

Keywords: thermoresponsive polymers, lower critical solution temperature (LCST), nanogels, drug delivery system, colchicine.

Contents

List of Figures	iii
List of Tables	iv
List of Abbreviations	v
1 Introduction	1
1.1 Scope of Research	2
1.2 Objectives	2
1.2.1 Principal Objective	2
1.2.2 Specific Objectives	2
1.3 Outline	3
2 Background Information	5
2.1 Polymeric Gels	5
2.2 Stimuli-Responsive Hydrogels	5
2.3 Biomedical Applications	6
2.4 Drug Delivery Systems (DDSs)	7
2.5 State-of-The-Art: Thermo-Responsive Polymers for Drug Delivery	9
3 Experimental Procedure	13
3.1 Reagents	13
3.2 Materials and Equipment	13
3.3 Synthesis of Hydrogels	14
3.3.1 Total Solids (TS) Analysis	15
3.4 Characterization and Methods	15
3.4.1 Dialysis	15
3.4.2 ATR-FTIR Spectroscopy	16
3.4.3 Cloud Point Determination	16
3.4.4 Particle Size Determination	16
3.4.5 High Pressure Liquid Chromatography (HPLC)	16
3.5 Drug Uptake Studies	17

3.6	Drug Release Studies	17
4	Results and Discussion	19
4.1	Synthesis	19
4.2	ATR-FTIR Studies	19
4.3	Thermo-responsiveness Studies	22
4.4	Particle Size Studies	23
4.5	Uptake and Release Studies	25
5	Conclusions and Recommendations	29
5.1	Conclusions	29
5.2	Recommendations	30
	References	31
	Attachments	37

List of Figures

2.1	Stimuli action of smart hydrogels. Taken from [26].	6
2.2	Drug concentration in the organism of drug delivery systems. Taken from [56].	8
2.3	Phase diagrams of thermo-responsive hydrogels with (a) UCST, and (b) LCST. Taken from [61].	9
2.4	Model transmittance curve as a function of temperature of LCST hydrogels. Taken from [61].	10
2.5	Chemical structures of (a) PNIPAM, and (b) PNVCL.	11
2.6	Dynamic hydration behavior of “sponge-like” PVCL mesoglobules. The light blue color represents the distribution density of water molecules. Taken from [65].	11
2.7	LCST polymer mechanism in drug delivery. Taken from [61].	12
2.8	Scheme of VCL-PEGDA _x synthesis.	12
3.1	Set-up for polymerization reaction.	14
3.2	Hydrogel purification by dialysis.	14
3.3	Steps for total solids analysis.	15
3.4	Steps of drug uptake.	18
3.5	Steps of drug release.	18
4.1	ATR-FTIR spectrum of VCL.	20
4.2	ATR-FTIR spectrum of PEGDA.	20
4.3	ATR-FTIR spectra of VCL-PEGDA _x	20
4.4	Resonance structures of PEGDA.	21
4.5	Chemical structures of (a) VCL-PEGDA ₀ , and (b) VCL-PEGDA _x (x=2,4,8).	22
4.6	Transmittance curves as a function of temperature for VCL-PEGDA _x	23
4.7	Calibration curve of colchicine (5-100 $\mu\text{g}/\text{mL}$).	25
4.8	Calibration curve of colchicine (2-20 $\mu\text{g}/\text{mL}$).	27
4.9	Cumulative release (%) of colchicine at $T = 38^\circ\text{C}$	27

List of Tables

2.1	Some examples of hydrogels for biomedical applications.	7
2.2	Examples of PNVCL-based nanocarriers.	12
3.1	Recipes for VCL-PEGDA _x syntheses.	14
4.1	Yield of VCL-PEGDA _x polymerization reactions.	19
4.2	Peak assignments for the ATR-FTIR of VCL, PEGDA, and VCL-PEGDA _x	21
4.3	LCST values for the VCL-PEGDA _x	22
4.4	Mean particle size and polydispersity index (PDI) of VCL-PEGDA _x at $T < LCST$	24
4.5	Mean particle size and polydispersity index (PDI) of VCL-PEGDA _x at $T > LCST$	24
4.6	Calibration curve parameters (5-100 $\mu\text{g/mL}$).	25
4.7	Drug Loading (% DL) and Encapsulation Efficiency (% EE) of VCL- PEGDA _x hydrogels.	26
4.8	Calibration curve parameters (2-20 $\mu\text{g/mL}$).	26

List of Abbreviations

AFM Atomic Force Microscopy

APS Ammonium persulfate, $(NH_4)_2S_2O_8$

CDDSs Conventional Drug Delivery Systems

DDI Distilled Deionized

DDSs Drug Delivery Systems

DL Drug Loading

DLS Dynamic Light Scattering

DSC Differential Scanning Calorimetry

EE Encapsulation Efficiency

HPLC High Performance Liquid Chromatography

IPN Interpenetrating Polymer Network

LCST Lower Critical Solution Temperature

MSU Monosodium urate

MWCO Molecular Weight Cut Off

NMR Nuclear Magnetic Resonance

NVCL N-vinylcaprolactam

PDI Polydispersity Index

PEGDA Poly(ethylene glycol) diacrylate

PNIPAM Poly(N-isopropylacrylamide)

SDS Sodium dodecyl sulfate, $NaC_{12}H_{25}SO_4$

SEM Scanning Electron Microscopy

TEM Transmission Electron Microscopy

UCST Upper Critical Solution Temperature

UV-vis Ultraviolet-visible

VPTT Volume Phase Transition Temperature

Chapter 1

Introduction

In modern society, the synthesis and characterization of polymeric gels show many advances due to the great variety of these materials in medicine and pharmacology fields, among others.[1] One important application lies in Drug Delivery Systems (DDSs). In this way, polymeric gels may be applied as carriers of active molecules in medical treatments inside and outside the human body, achieving a reduction of adverse effects and, at the same time, increment biocompatibility to the patient. [2, 3]

Since the therapeutic effectiveness of a DDS is dependent on the administration method, choosing one or another method relies on the drug efficacy related to their absorption, distribution, metabolism, and excretion (ADME) process profiles. Oral administration is generally the Conventional Drug Delivery System (CDDS). This administration method releases immediately, so drug absorption in the body is relatively rapid and requires frequent doses of the drug. Repeated doses show some limitations because the drug level in the blood increases after each dose, and then decreases until the subsequent drug administration.[5]

For that reason, some specific polymers are attracting considerable interest due to their capability to reduce the drug administration doses. Thereby, the drug is released at a constant rate over prolonged periods and always inside the therapeutic level. An important advantage of controlled drug release is durability, that is, the lasting for days to years without degradation at normal environmental conditions. Controlled DDSs offer many other advantages such as better efficacy, less toxicity, and improved patient compliance and convenience. [6, 7]

Controlled DDSs do not pretend to displace other ways of drug administration but finding primary usefulness in specific controlled therapies and prophylactic situations.[8]

For example, the accumulation of monosodium urate (MSU) crystals in the articulations and the surrounding tissues causes gout disease. The first choice to prevent and treat gout is the prophylactic drug called colchicine. Nevertheless, it is strongly toxic and presents a low therapeutic index for humans. [9–11]

In the field of nanomedicine, since 2015, the use of stimuli-responsive nano-scale hydro-

gels (nanogels) as carriers for DDSs have received much attention. [12] Among stimuli-responsive nanogels, those sensitive to temperature and pH have received significant attention as smart DDSs due to their ability to suffering reversible phase transitions in response to the stimuli changes in the medium. [13–16]

1.1 Scope of Research

This study aimed to further the current knowledge of polymeric nanogels for Drug Delivery Systems (DDSs) evolving from two aspects: (1) stimuli-responsive nanogels have been taking great importance in nanomedicine, and (2) some drugs show low therapeutic index.

This research focuses on the synthesis of smart polymers based on N-vinyl caprolactam crosslinked with poly(ethylene glycol) diacrylate, which presents biocompatibility and thermo-responsiveness. The model medicine for release studies is colchicine, a drug currently in disuse because of its low therapeutic index. Thereby, a controlled DDS for this drug can help to stabilize the drug concentration in the bloodstream, and minimize the dose frequency, obtaining a safer drug administration.

1.2 Objectives

1.2.1 Principal Objective

The main objective is to analyze the drug delivery profile of colchicine released from VCL-PEGDA based hydrogels.

1.2.2 Specific Objectives

- To carry out the synthesis of PNVCL and VCL-PEGDA-based nanogels.
- To characterize the obtained polymers by means of techniques, such as total solids, cloud point, DLS, and FTIR.
- To evaluate thermo-responsiveness of hydrogels.
- To quantify drug loading and release by HPLC analytical method.
- To compare the influence of crosslinker in drug loading and release.
- To compare the drug release profile of these polymers against similar systems.

1.3 Outline

This study is divided into five chapters. The first chapter presents the thesis' topic, specifies the scope of research, and enumerates the general and specific objectives. The second chapter gives an overview of the background information about hydrogels and its biomedical application in the Drug Delivery Systems (DDSs), describing some of their properties, and known information about VCL-PEGDA hydrogels. Chapter 3 describes the experimental procedure used for the thesis development, including the information of reagents, materials, equipment, synthesis process, characterization methods, and drug uptake/release. Chapter 4 looks at the analysis of the results and discussion. Finally, conclusions and recommendations are summarized in Chapter 5.

This page is intentionally left blank.

Chapter 2

Background Information

2.1 Polymeric Gels

According to the Encyclopedia of Polymer Science and Engineering, a polymeric gel is a three dimensional (3D) network constituted of a cross-linked polymer swollen in a solvent. They present one or more unique properties, such as infinite molecular weight, insolubility, non-fusibility, or reversible swelling ability, and they depend exclusively on polymer-solvent interactions.[17]

The term hydrogel has been used to refer to polymeric gels constituted of at least one hydrophilic component making it soluble in water,[18] and they can be classified in many ways by [19]:

- Source: natural or synthetic.
- Physical state: solid, semisolid, or liquid.
- Polymeric composition: homopolymeric, copolymeric, or multi-polymeric (also referred as Interpenetrating Polymer Network (IPN))
- Configuration: crystalline, semi-crystalline, or amorphous.
- Cross-linking types: physical or chemical.
- Degradability: biodegradable or not.
- Ionic charge: cationic, anionic or non-ionic.
- Particle size: macrogel, microgel, or nanogel.

2.2 Stimuli-Responsive Hydrogels

The swelling allows to hydrogel absorbing a water volume, which penetrates the gel matrix causing that gel-solvent interactions are stronger than gel-gel interactions. Nevertheless, it does not mean that the water explicitly dissolves the polymer. This swelling property comes from hydrophilic functional groups of the polymeric backbone; meanwhile their resistance to dissolution comes from the crosslinked network chains. In the literature, the term 'colloidal gels' is generally understood as a type of hydrogel in which dispersion

medium is water.[20–23]

Dušek and Patterson [24] argued that it is possible to control the swelling property reversibly with external condition changes, such as physical or chemical stimuli (Figure 2.1). Accordingly, there has been considerable interest in the study of stimuli-responsive hydrogels, so-called 'intelligent/smart hydrogels'.[25]

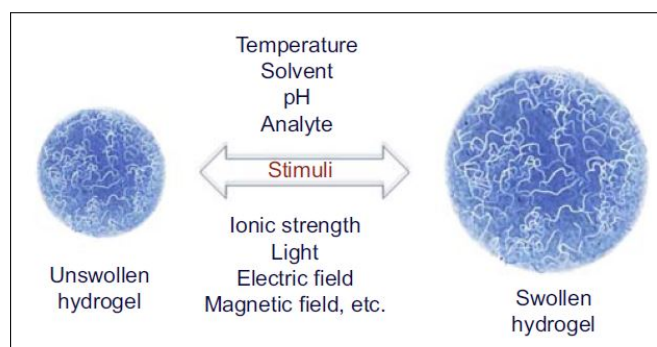


Figure 2.1: Stimuli action of smart hydrogels. Taken from [26].

In the literature, there are a surprising number of studies about the different types of stimuli, being physical, chemical, dual, or biochemical. Stimuli as temperature [27, 28], light [29, 30], electric [31, 32] or magnetic field [33, 34] refers to physical responses; whereas pH [35, 36], ionic strength [37, 38], and presence of molecular species such as glucose [39, 40] are part of chemical stimuli-responses. The dual response for which a combination of two stimuli-responses (such as pH combined with temperature) occurs is nowadays receiving much attention. [41, 42] Further, biochemical stimulus-responses occur when biological agents [43, 44] as ligands, enzymes, or antigens are involved.

2.3 Biomedical Applications

Additional to stimuli-responsiveness, the retention of high amounts of water provides consequently properties such as permeability, storage capability, bio-compatibility, functionality, and non-toxicity; making hydrogels potential materials for biomedical applications.[21] For example, the water-solubility and bio-compatibility make hydrogels very suitable for tissue or artificial organ implants due to the considerable reduction of friction between an implanted biomaterial and its surrounding tissues.[45, 46] Likewise, swelling in response to an environmental change and storage capability make hydrogels perfect candidates for controlled release systems.[45] More examples of biomedical applications are presented in Table 2.1.

Table 2.1: Some examples of hydrogels for biomedical applications.

Biomedical application	Example	Ref.
Drug delivery	Poly(vinylcaprolactam)-based biodegradable multiresponsive microgels for drug delivery.	[47]
Tissue engineering	Degradable, thermo-sensitive Poly(N-isopropyl acrylamide)-based scaffolds with controlled porosity for tissue engineering applications.	[48]
Biosensors	Hydrogel with chains functionalized with carboxyl groups as universal 3D platform in DNA biosensors.	[49]
Self-healing	pH responsive self-healing hydrogels formed by boronate-catechol complexation.	[50]
Actuators	Novel hydrogel actuator inspired by reversible mussel adhesive protein chemistry.	[51]

2.4 Drug Delivery Systems (DDSs)

Conventional Drug Delivery Systems (CDDSs), such as oral, topical, trans-mucosal, parenteral, and inhalation routes, are traditionally used for drug administration. Nevertheless, they present many limitations because their relatively rapid drug absorption requires repeated doses of the drug. [5]

In an attempt to suggest alternatives, the first release formulation for controlling drug release kinetics was developed by Smith Klein Beecham in 1952. [52] Accordingly, several advances in the development of targeted, controlled, and modulated drug delivery systems have been taking place. Indeed, the first liposome nanoparticle for targeted drug delivery was developed by Peter Paul Speiser in 1960. [53] Subsequently, the use of polymeric nanoparticles (also named nanogels) for controlled release systems has been extensively investigated.[20] Since 2015, investigations on site-specific targets and stimuli-responsive nanogels have become of great interest. [12]

The polymeric matrix is capable of protect the drug from hostile environments, such as low pH or enzymes, and also, they can control the drug liberation when the hydrogel structure changes in response to a stimulus. [54] Additionally, they present low interfacial tension, so the proteins of the body fluids are not absorbed easily. This characteristic allows the loading of different sized molecules and their release effortlessly through many administration routes.[55] For these reasons, smart hydrogels present many advantages in the following situations:

- A sustained constant concentration of the drug in the body system is desired.
- The bio-active compound has a very short half-time.
- The drug has strong side-effects or stability problems.
- It is necessary to achieve a better patient compliance.
- The drug is wasted or taken in frequent dosage.

In terms of drug release rates, DDSs generally show five release profiles [56]:

- Type I is the conventional release rate when the drug enters the body and is rapidly released.
- Type II (zero-order profile) produces a constant drug release along time since the drug enters the body.
- Type III produces a constant release rate, but in this case, exists a delay of starting drug delivery.
- Type IV shows drug liberation at a specific time, i.e., during the night.
- Type V displays a constant release of a therapeutic agent for short-lasting spans, i.e., liberating hormones for three days/month for consecutive months.

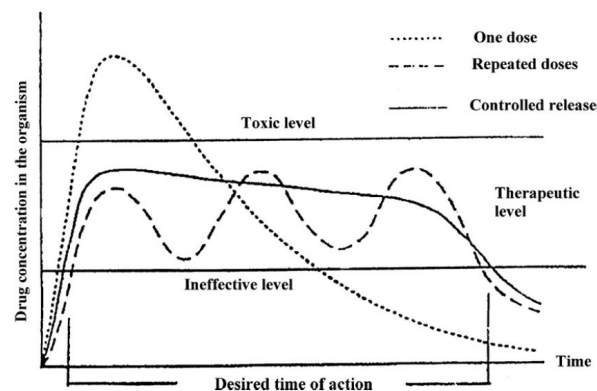


Figure 2.2: Drug concentration in the organism of drug delivery systems. Taken from [56].

The profile of greater interest for controlled drug delivery is type II, which corresponds to a zero-order release rate exhibiting a constant drug concentration in the body over time (Figure 2.2). Nevertheless, some fluctuations in drug concentration levels can occur because the drug solubility in tissues also determines its absorption.[56]

2.5 State-of-The-Art: Thermo-Responsive Polymers for Drug Delivery

As mentioned earlier, stimuli-responsive hydrogels are excellent candidates for designing controlled DDSs. Recently, pH- or thermo-responsive are the most studied due to its physiological importance. This work is focused on thermo-responsive hydrogels since they can take advantage of the temperature difference between environment, body (37 °C), presence of fever (>37.5 °C), or presence of an intratumoral environment (40–44 °C). [57, 58] For these reasons, they have an excellent performance for cancer therapy [58], transdermal drug therapy [42], and oral drug delivery [59].

Thermo-sensitive hydrogels exhibit a phase transition when there is a change in temperature, so gel volume increases or decreases depending on having a Upper Critical Solution Temperature (UCST) or Lower Critical Solution Temperature (LCST).[60]

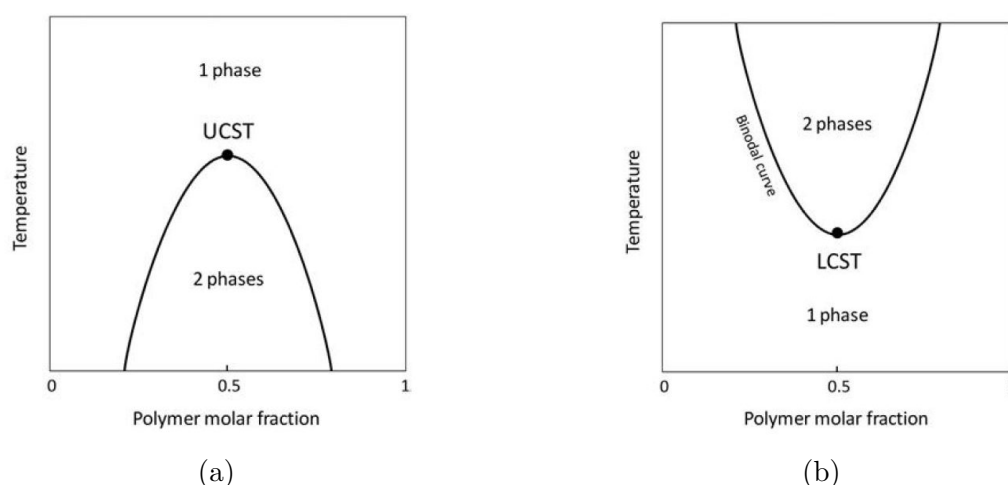


Figure 2.3: Phase diagrams of thermo-responsive hydrogels with (a) UCST, and (b) LCST. Taken from [61].

In general, UCST hydrogels are water-insoluble below the critical temperature, so the aggregate state predominates (two-phase region). Upon heating, the polymer begins to dissolve until it is entirely miscible (single-phase region) (Figure 2.3a). The temperature at which solvation starts is named UCST.[62]

On the other hand, LCST hydrogels present a phase separation when heating the system above a specific temperature named LCST (Figure 2.3b). Below LCST, the polymer chains interact with water by H-bonding, so, the hydrogen bond energy predominates in the system, and the polymer is miscible in the water showing a swollen state (single-

phase). Upon heating, the hydrogen bond interactions become weaker, while polymer-polymer hydrophobic interactions become stronger due to the molecular agitation, and polymer phases out of the solution. That phase transition occurs particularly at LCST, also called the cloud point, which is visually perceptible because the solution passes from transparent to turbid (Figure 2.4). Above LCST, polymer-water interactions are broken, causing a phase separation, and a reduction of the polymer volume. For that reason, the term Volume Phase Transition Temperature (VPTT) is used to refer to this phase transition temperature, too.[63]

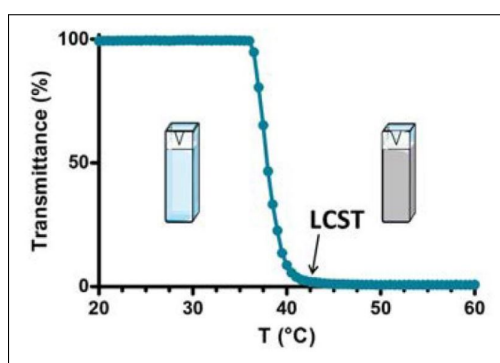


Figure 2.4: Model transmittance curve as a function of temperature of LCST hydrogels. Taken from [61].

The most common LCST hydrogels are those natural or synthetic containing functional groups in their side chains like hydroxyl, amine, amide, ether, carboxylate, or sulfonate.[55] Presently, one of the synthetic hydrogel most studied is the poly(*N*-isopropyl acrylamide) (PNIPAM), which is a vinyl polymer with secondary amide pendant groups (Figure 2.5a), and shows a VPTT near 32 °C. However, this polymer induces cellular cytotoxicity at 37 °C, and the secondary amide group can produce toxic amines if hydrolysis occurs. Consequently, is not biocompatible.[64] For this reason, it has been a challenge to develop a biocompatible thermo-responsive hydrogel, and poly(*N*-vinyl caprolactam) (PNVCL) based polymers are considered a good alternative to PNIPAM for controlled drug delivery systems.

Similarly to PNIPAM, PNVCL shows a LCST near 32 °C. Additionally, Vihola et al. [64] have been demonstrated that cell cultures successfully tolerated PNVCL polymer after three hours of incubation, at concentrations in the range 0.1–10.0 mg/ml, at both room and physiological temperature (37 °C).

The chemical structure of PNVCL (Figure 2.5b) shows an amide group directly connected

to the backbone of the polymer, allowing to improve its biocompatibility because toxic low-molecular-weight amines are not produced during hydrolysis. [45, 65]

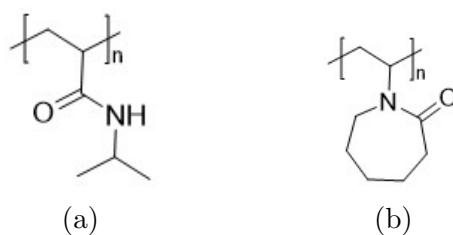


Figure 2.5: Chemical structures of (a) PNIPAM, and (b) PNVCL.

Sun and Wu [65] demonstrated the dynamic hydration behavior of PNVCL. In this way, the two lone pairs of the oxygen atom and the lone pair of nitrogen are acceptors of hydrogen bonds, so H-bonding interaction occurs below LCST. According to the literature, the energy of a hydrogen bond is mainly governed by temperature. For instance, when the temperature rises, the molecular agitation makes H-bonding unstable, and hydrogen bonds are weaker.[66] Above LCST, the hydrophobic effect increases and becomes predominant, so the polymer phases out from the solution and aggregates. Upon heating, the result is a "sponge-like" structure consisting of a hydrophobic core and a hydrophilic surface.[65] The phase transition behavior of PNVCL is illustrated in Figure 2.6.

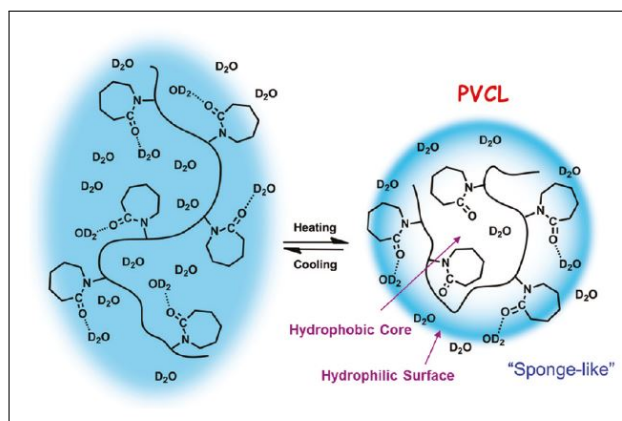


Figure 2.6: Dynamic hydration behavior of "sponge-like" PVCL mesoglobules. The light blue color represents the distribution density of water molecules. Taken from [65].

In this way, LCST polymers are excellent candidates to design polymeric particles for controlled, targeted, and sustained drug delivery on the nanometric scale, also called nanocarriers.[67] The release mechanism for drug delivery consists of (1) the encapsulation at temperatures below LCST, and (2) the delivery when the polymer shrinks at a temperature above LCST. Recently, many researchers have been working on the devel-

opment of hydrogels based on PNVCCL because of the reversible volume transition from micro- to nano-scale, as illustrated in Figure 2.7.[67] Some examples of this type of polymer are listed in Table 2.2.

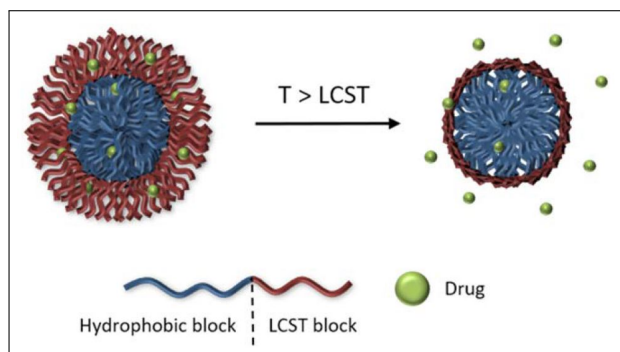


Figure 2.7: LCST polymer mechanism in drug delivery. Taken from [61].

Table 2.2: Examples of PNVCCL-based nanocarriers.

Polymer	Nanocarrier	Application	Ref.
P(NVCL-co-AGA)	Nanogel	Controlled drug release	[68]
fib-g-PNVCL	Nanogel	Controlled drug release	[69]
PE-PCL-b-PNVCL-FA	Micelle	Targeted and On-Demand drug release	[70]
P(NVCL-co-HEMA)	Nanogel	Controlled drug release	[71]

This work aims to synthesize PVCL-based polymers to obtain suitable nanocarriers for drug delivery applications. PEGDA is the chosen crosslinker due to its biocompatibility, hydrophilicity, and ability to prevent protein adsorption and cell adhesion.[72] Imaz and Forcada [63, 73] reported a synthetic procedure to obtain poly(VCL-co-PEGDA) microgels by emulsion polymerization (Figure 2.8). In the present work, the model drug for drug release studies is colchicine due to the important application for gout treatment and its low therapeutic index,[4] which motivates overcome this limitation.

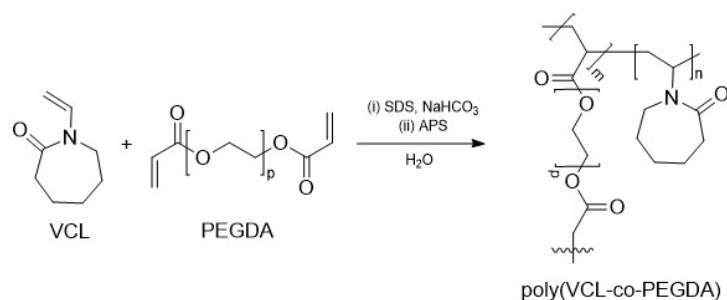


Figure 2.8: Scheme of VCL-PEGDAx synthesis.

Chapter 3

Experimental Procedure

3.1 Reagents

N-vinylcaprolactam (VCL; Sigma Aldrich, 98%), Poly(ethylene glycol) diacrylate (PEGDA; Sigma Aldrich, Mn 250), ammonium persulfate (APS; FMC Corporation, >99%), sodium dodecyl sulfate (SDS; STEOL® CS-230 Stepan), sodium hydrogen carbonate (Sigma Aldrich, $\geq 99.7\%$), colchicine (Sigma Aldrich, $\geq 95\%$), potassium dihydrogen phosphate (Fisher Scientific, 99.6%), and methanol (LiChrosolv®, HPLC grade) used as provided. All aqueous solutions were prepared with double deionized water (DDI) produced by a *Direct-Q® 3 UV Water Purification System*.

3.2 Materials and Equipment

Materials		
Flat bottom flask	50 mL glass recipients	Graham condenser
Graduated cilinder	Glass pasteur pipettes	10 mL test tubes
10 mL, 25 mL volumetric flasks	Vials	Petri dishes

Equipment	Specifications
Micropipettes	<i>Thermo™ Scientific™ Finnpiquette F1 Fixed Volume TS1000H Topscien</i>
Hot plate stirrer	<i>MS300HS M TOPS</i>
Analytical balance	<i>HR-150A Cobos precision</i>
Heating cleaning bath	<i>Ultrasons-HD. J.P. SELECTA</i>
Drying oven	<i>SLN 115 POL-EKO-APARATURA</i>
pH-meter	<i>HI2002-02 HANNA Instruments</i>
with glass electrode	<i>HI11310 HANNA Instruments</i>
Thermometer	<i>PROMOLAB® Economy</i>
Electronic thermometer	<i>WT-2 Elitech</i>
UV-vis spectrophotometer	<i>ZUZI® 4211/50</i>
FTIR spectrometer	<i>Agilent Cary 630</i>
Particle size analyzer	<i>BI-90 Plus Brookhaven Instrument Corporation</i>
HPLC apparatus	<i>UltiMate 3000</i>
C-18 column for HPLC	<i>Hypersil GOLD™ (150 mm× 4.6 mm, 5μ particle size)</i>
Dialysis membrane	<i>Carolina™ Dialysis Tubing (MWCO: 12'000 - 14'000)</i>

3.3 Synthesis of Hydrogels

Four thermo-responsive poly(N-vinyl caprolactam-co-PEGDA) (poly(VCL-co-PEGDA)) hydrogels were synthesized by emulsion polymerization of VCL and PEGDA in a flat bottom flask equipped with a reflux condenser (Figure 3.1), using PEGDA as a crosslinker, SDS as emulsifier, APS as initiator, and sodium hydrogen carbonate as buffer. Once the monomer, the crosslinker, the emulsifier, and the buffer were charged, the system was heated to 70 °C and stirred at 350 rpm. Then, the initiator was added, and after a short period of time, the reaction system became turbid showing that polymerization started. The reaction was allowed to continue for 7h with stirring and 70 °C. Once polymerization finished, the reaction was allowed to cool down to room temperature, and stirring continued for 12 h to avoid agglomeration. The final products were dialyzed against DDI water at least three times a day to remove non-reacted reagents and impurities until solvent showed conductivity of DDI (1.7 μS) (Figure 3.2). Recipes and reaction conditions are resumed in Table 3.1.

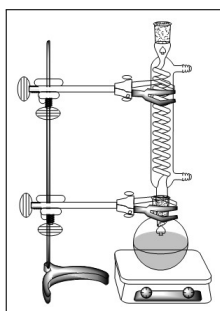


Figure 3.1: Set-up for polymerization reaction.

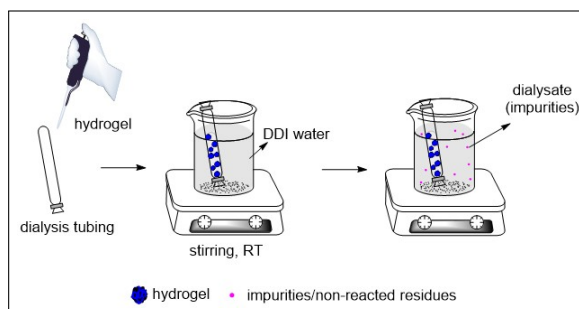


Figure 3.2: Hydrogel purification by dialysis.

Table 3.1: Recipes for VCL-PEGDA_x syntheses.

Code	PEGDA (<i>wt %VCL</i>)
VCL-PEGDA0	–
VCL-PEGDA2	2
VCL-PEGDA4	4
VCL-PEGDA8	8

Reaction conditions: rpm= 350; t= 7h; T= 70°C.

The concentration of VCL was 2.0 wt%.

The concentration of initiator was 0.7 wt% VCL.

The concentration of buffer and emulsifier were 1.7 wt% VCL.

3.3.1 Total Solids (TS) Analysis

Concentration of hydrogels were estimated by Total Solids (TS) analysis by weighing the amount of solid present in a known volume of purified hydrogel.

The analysis was carried out by weighing a Petri dish, filling it with a known volume of hydrogels, and evaporating the water in a drying oven at 105 °C during 2 h to constant weight. Finally, the Petri dish was weighted, and concentration (C) of purified hydrogels was calculated by Equation 3.3.1:

$$C (wt\%) = \left(\frac{m_f - m_i}{V} \right) \cdot 100 \quad (3.3.1)$$

where m_i is the weight of the empty Petri dish, m_f is the weight of Petri dish with residual gel, and V is the volume of hydrogel added. Procedure was illustrated in Figure 3.3.

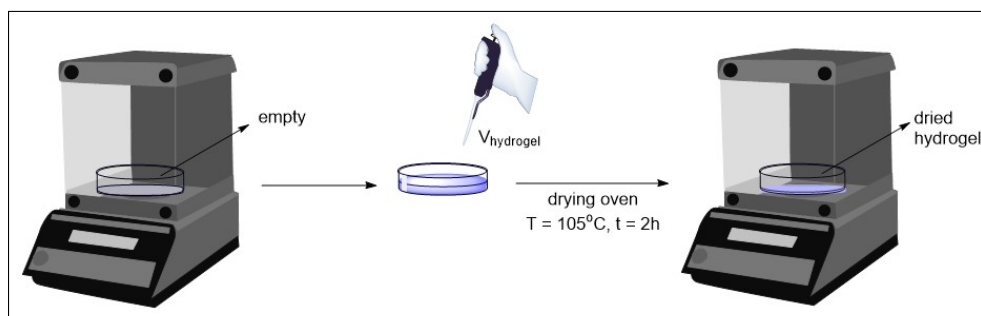


Figure 3.3: Steps for total solids analysis.

The yield of polymerization was calculated gravimetrically by Equation 3.3.2:

$$\% \text{ yield} = \left(\frac{C_{TS}}{C_{TS, \text{theoretical}}} \right) \cdot 100 \quad (3.3.2)$$

where C_{TS} is the concentration of hydrogels obtained from Total Solids analysis, and $C_{TS, \text{theoretical}}$ is the theoretical Total Solids of hydrogels showed in Attachment C.

3.4 Characterization and Methods

3.4.1 Dialysis

Purification of hydrogels and drug uptake/delivery systems were carried out by dialysis against DDI water using Carolina™ Dialysis Tubing (MWCO: 12'000 - 14'000) as dialysis membrane.

3.4.2 ATR-FTIR Spectroscopy

Polymer characterization were examined by ATR-FTIR spectroscopy. Measurements were carried out for VCL-PEGDAx hydrogels, VCL, and PEGDA dried samples.

3.4.3 Cloud Point Determination

The cloud point (or LCST) of hydrogels was determined by UV-vis spectrophotometry monitoring the light transmittance of the hydrogel upon cooling the hydrogels from 40°C until room temperature. The measurements were performed at 650 nm to avoid the absorbance of light. The temperature was recorded with a digital thermometer.

3.4.4 Particle Size Determination

The mean particle diameters of hydrogels' aqueous dispersion were measured by Dynamic Light Scattering (DLS) method using a particle size analyzer. The device was equipped with a solid-state (35 mW) standard laser and wavelength of 659 nm light-source. All measurements were carried out five time at two temperatures (RT and T>LCST) five times at each temperature to give an average hydrodynamic diameter and size distribution. The plastic cuvette was filled with approximately 1 mL of the hydrogels previously purified by dialysis. The mean particle diameter and polydispersity index (PDI) parameters were calculated using *ZetaPlus Particle Sizing Software*. Two Nanosphere™ size standards were used: (1) 90 nm (*Duke Scientific Corporation*), and (2) 20 nm (*Thermo Scientific*).

3.4.5 High Pressure Liquid Chromatography (HPLC)

A HPLC apparatus equipped with an autosampler, a quaternary pump, a column compartment, and a UV-vis detector was used as drug uptake/release analytical method. The analysis was carried out using a reverse phase C-18 column. The mobile phase was prepared as [74], mixing potassium dihydrogen phosphate (450 mL, 6.8 g/L) and methanol (530 mL). The mix cooled down to room temperature and the mixture was completed to 1000 mL with methanol. Then, pH was adjusted to 5.5 with diluted phosphoric acid. The final mixture was filtered through *Titan 47 mm Membrane Disc* filters. The flow rate of the mobile phase was 1.0 mL/min and the injection volume was 20 µL. The column temperature was kept at 30 °C, and detection was carried out at 254 nm.

Standard solutions and calibration curves

A standard stock solution of colchicine (1000 $\mu\text{g}/\text{mL}$) was prepared. From this stock solution, standards with concentrations of 2, 5, 15, 16, 20, 40, 65, 100 $\mu\text{g}/\text{mL}$ were also prepared. Two calibration curves were constructed over the concentration ranges of 2-20 and 5-100 $\mu\text{g}/\text{mL}$, both with five concentration levels. *Chromeleon™ Chromatography Data System Software* was used in order to obtain the corresponding calibration curves.

3.5 Drug Uptake Studies

The drug loading procedure is shown in Figure 3.4. The method used was to take 9 mL of hydrogel, placed in a 50 mL glass recipient, and dried at 50 °C. The dried hydrogel was allowed to swell in 5 mL of drug solution (1000 $\mu\text{g}/\text{mL}$). The mixture was sonicated for 20 min at RT, and rested for 48 h in order to reach equilibrium. Then, the mixture was subjected to dialysis overnight in order to remove the non-loaded drug from the system. Posteriorly, the dialysate solvent was recollected, filtrated with 0.45 μm syringe filters, and quantified by the analytical method previously described in Section 3.4.5. Thus, the % of drug loading (DL) and encapsulation efficiency (EE) was determined using Equations 3.5.3 and 3.5.4, respectively, where $m_{hydrogel}$ is the mass of hydrogel in the encapsulation process, $m_{actual\ loading}$ is the encapsulated drug, and $m_{theoretical\ loading}$ is the total amount of drug initially added.

$$\% DL = \left(\frac{m_{actual\ loading}}{m_{hydrogel}} \right) \cdot 100 \quad (3.5.3)$$

$$\% EE = \left(\frac{m_{actual\ loading}}{m_{theoretical\ loading}} \right) \cdot 100 \quad (3.5.4)$$

3.6 Drug Release Studies

The previously dialyzed mixture was placed in a dialysis membrane, and again dialyzed to release the drug against DDI water (35 mL) at 38 °C approximately (Figure 3.5a). At regular intervals of time, dialysates containing the released drug were collected in test tubes (Figure 3.5b). After every sample collection, the solvent was refreshed (Figure 3.5c). Finally, all recollected samples were filtered with 0.45 μm syringe filters, and quantified by the HPLC analytical method previously described in Section 3.4.5.

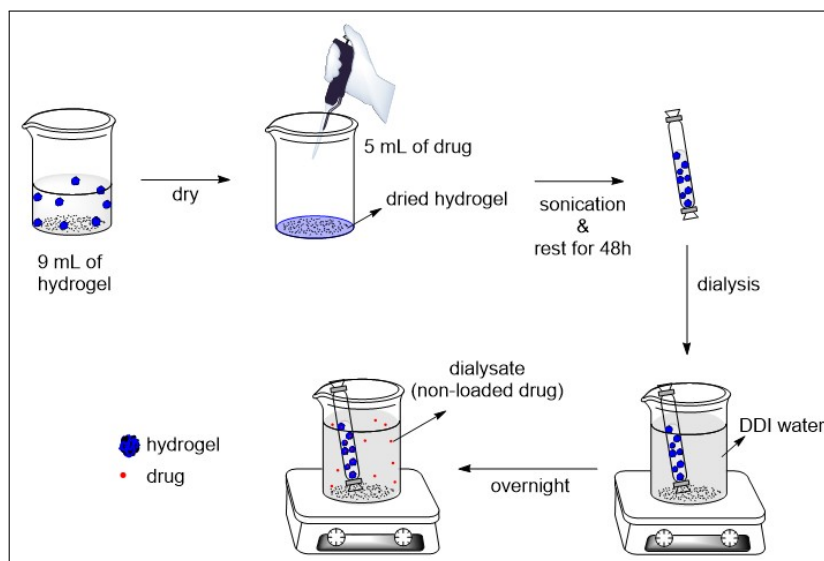


Figure 3.4: Steps of drug uptake.

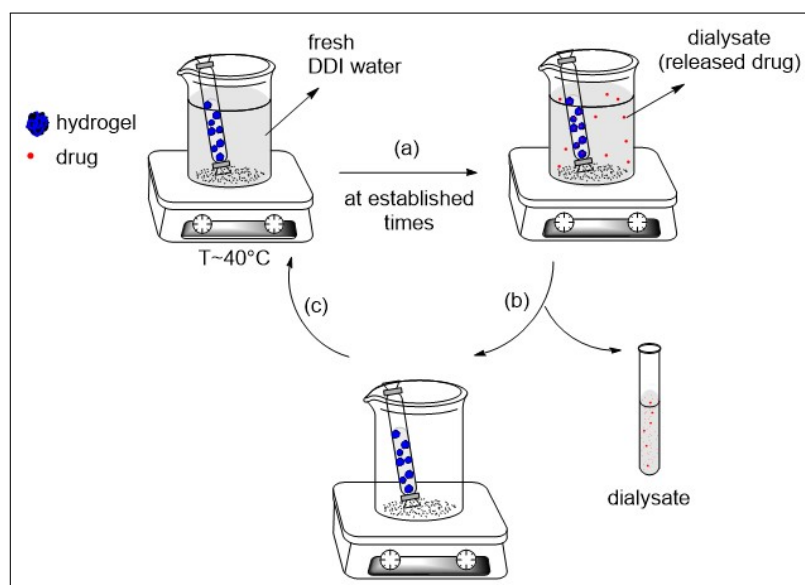


Figure 3.5: Steps of drug release.

Chapter 4

Results and Discussion

4.1 Synthesis

Four poly(VCL-co-PEGDA) reversible water-soluble hydrogels were synthesized by emulsion polymerization with different crosslinker amounts (0, 2, 4, 8 wt%) relative to the VCL monomer. During the reactions, the appearance of turbidity was observed with the addition of the APS initiator, showing that polymerization started. After 7 h of reaction, the polymers were cooled down, and turbidity slowly disappeared. The transition to transparency from turbidity confirmed that volume phase transition had occurred, and the resulting polymer materials were thermo-responsive.[75] Once polymerization had been finished, the hydrogels were purified by dialysis to remove non-reacted reagents until dialysate showed conductivity of DDI water ($1.7\mu S$), approximately.

Total Solids (TS) were computed to know the actual concentration of hydrogels using Equation 3.3.1. Also, theoretical TS values (Attachment C) were calculated to know the polymerization yield from Equation 3.3.2. The obtained values show relatively good yields from $(55.8 \pm 0.3) \%$ to $(75.0 \pm 2.4) \%$ (Table 4.1).

Table 4.1: Yield of VCL-PEGDAx polymerization reactions.

	$TS_{experimental} (wt/V\%)$	$TS_{theoretical} (wt/V\%)$	$\% yield$
VCL-PEGDA0	1.50 ± 0.02	2.086 ± 0.001	71.8 ± 1.1
VCL-PEGDA2	1.24 ± 0.01	2.215 ± 0.001	55.8 ± 0.3
VCL-PEGDA4	1.65 ± 0.05	2.202 ± 0.001	75.0 ± 2.4
VCL-PEGDA8	1.50 ± 0.01	2.342 ± 0.001	63.8 ± 0.6

4.2 ATR-FTIR Studies

The chemical structure of the poly(VCL-co-PEGDA) hydrogels was confirmed by ATR-FTIR spectroscopy. The spectra of VCL, PEGDA, and VCL-PEGDAx are shown in Figure 4.1, Figure 4.2, and Figure 4.3, respectively. The characteristic peaks of VCL monomer, PEGDA crosslinker and VCL-PEGDAx ($x = \%$ crosslinker amount) hydrogels are listed in Table 4.2.

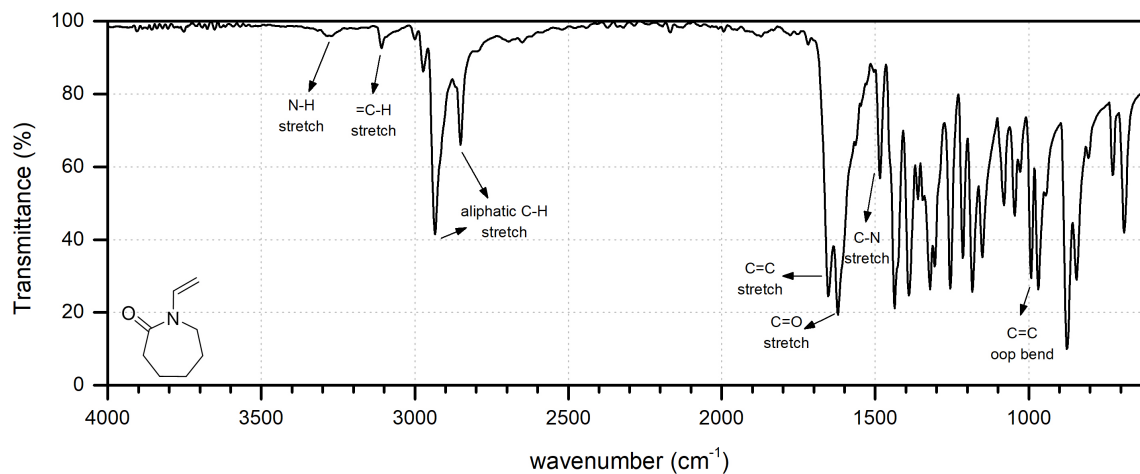


Figure 4.1: ATR-FTIR spectrum of VCL.

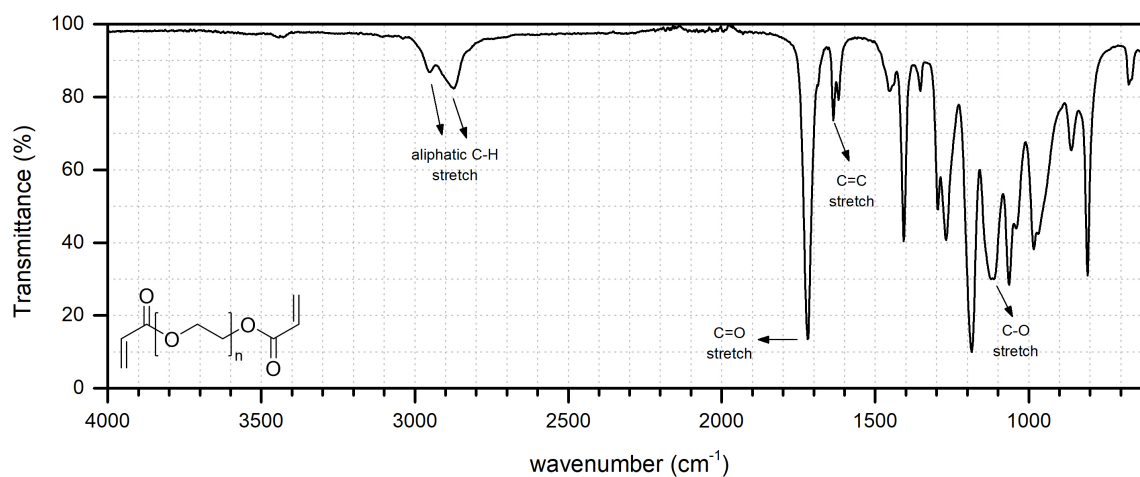


Figure 4.2: ATR-FTIR spectrum of PEGDA.

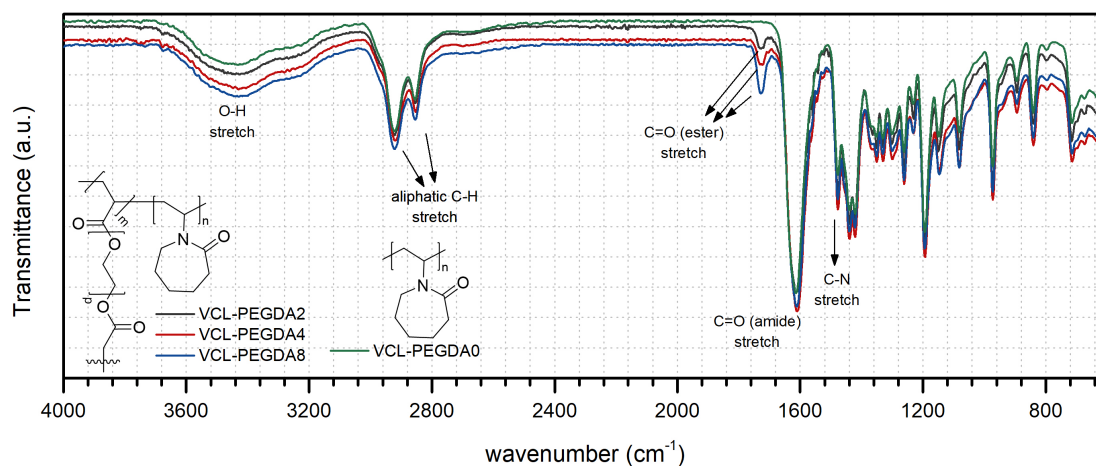
Figure 4.3: ATR-FTIR spectra of VCL-PEGDA_x.

Table 4.2: Peak assignments for the ATR-FTIR of VCL, PEGDA, and VCL-PEGDA_x.

	shift (cm ⁻¹)					
	=C-H	C=C	C=O (amide)	C=C (oop)	C=O (ester)	O-H
VCL	3160	1659	1621	992	–	–
PEGDA	–	1636	–	–	1719	–
VCL-PEGDA0	–	–	1610	–	–	3428
VCL-PEGDA2	–	–	1612	–	1727	3426
VCL-PEGDA4	–	–	1610	–	1730	3429
VCL-PEGDA8	–	–	1611	–	1729	3429

In the FTIR spectrum of the monomer VCL (Figure 4.1), it can be observed the characteristic vinyl peaks of =C-H stretching at 3160 cm⁻¹, and C=C stretching at 1659 cm⁻¹. The characteristic peak of carbonyl (C=O) stretching for an amide group is generally found at 1700-1640 cm⁻¹. Cyclic amides (lactams) decreases the C=O frequency for increasing ring size. Indeed, in the monomer spectrum, C=O is shown at a lower frequency (1621 cm⁻¹) due to the 7-membered lactam.

Figure 4.2 shows the characteristic peaks of the crosslinker PEGDA. In general, the C=O stretching band of an ester group appears at 1750-1735 cm⁻¹. Conjugation of the carbonyl group with α, β unsaturations shifts the stretching C=O vibration by about 15 to 25 cm⁻¹ to lower frequencies, and C=C vibration to lower frequency, too. For that reason, the C=O band of the ester groups is found at 1719 cm⁻¹ and C=C stretching band at 1636 cm⁻¹. Resonance structures of PEGDA are shown in Figure 4.4.

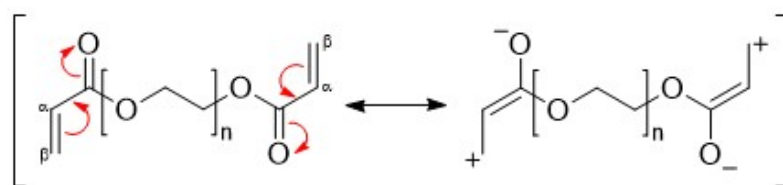


Figure 4.4: Resonance structures of PEGDA.

The FTIR spectra of VCL-PEGDA_x hydrogels are shown in Figure 4.3. VCL-PEGDA0 corresponds to the poly(N-vinyl caprolactam) (PVCL) homopolymer without crosslinker (Figure 4.5a), while VCL-PEGDA_x (x=2,4,8) corresponds to the poly(VCL-co-PEGDA) hydrogels (Figure 4.5b).

Four spectra showed the absence of C=C stretching (1659 cm⁻¹), =CH stretching (3100 cm⁻¹), and C=C out-of-plane bending (992 cm⁻¹) in comparison to monomer VCL spectrum indicating that polymerization occurred. The intense C=O stretching band of the

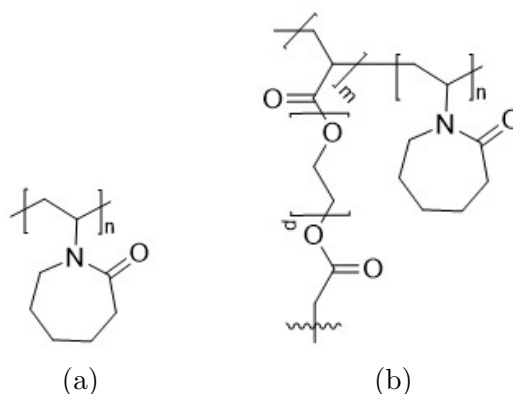


Figure 4.5: Chemical structures of (a) VCL-PEGDA0, and (b) VCL-PEGDA_x (x=2,4,8).

VCL amide group is shown at $\sim 1610\text{ cm}^{-1}$, and the C-N stretching at $\sim 1477\text{ cm}^{-1}$ in all spectra. Both peaks showed a displacement to lower frequencies in comparison to monomer VCL that might be due to the changes in the conformation of the molecules and interaction of molecules upon polymerization.

Crosslinking of VCL-PEGDA_x (x=2,4,8) cannot be confirmed by the absence of vinyl peaks because possible overlapping due to the low concentration of PEGDA. Thus, the C=O (ester) stretching band at $\sim 1730\text{ cm}^{-1}$ and its displacement to higher frequency indicates the absence of conjugation, and it could demonstrate the crosslinking of VCL-PEGDA hydrogels.

4.3 Thermo-responsiveness Studies

During the synthesis process, copolymers showed a phase transition from turbid to transparent solutions when cooling down. For this reason, turbidity measurements were carried out to estimate the cloud point temperatures (also called LCST) of hydrogels at 650 nm. Figure 4.6 shows the transmittance curves of VCL-PEGDA_x hydrogels, and Table 4.3 resumes the LCST values of hydrogels.

Table 4.3: LCST values for the VCL-PEGDA_x.

	LCST ($\pm 0.1^\circ\text{C}$)
VCL-PEGDA0	32.0
VCL-PEGDA2	32.7
VCL-PEGDA4	32.6
VCL-PEGDA8	32.3

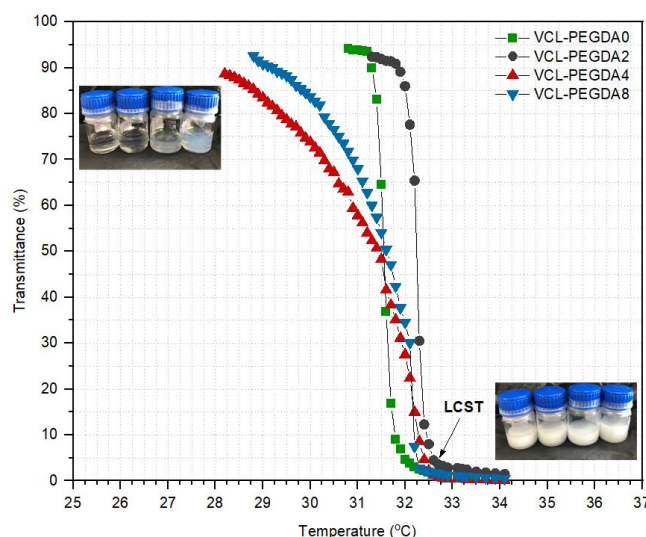


Figure 4.6: Transmittance curves as a function of temperature for VCL-PEGDA_x.

According to the literature, the LCST can be defined as the temperature at which the polymer solution becomes turbid, so it has a transmittance closer to 0%. For poly(*N*-vinyl caprolactam) (PNVCL), the LCST value is reported between 30-32 °C and is slightly impacted by the concentration. On the other hand, polyethylene glycol (PEG) derivatives manifest an LCST at 90 °C in water. Although, their use as a crosslinker helps to exhibit a relevant LCST.[61, 76]

In general, the crosslinker concentration slightly influences on the LCST values. During the experiment, PNVCL (VCL-PEGDA0) showed a sharp phase transition with $(32.2 \pm 0.1)^\circ\text{C}$ LCST value, which is in good agreement with literature.[67] VCL-PEGDA2 showed a similar phase transition behavior but higher LCST value $(32.7 \pm 0.1)^\circ\text{C}$, while VCL-PEGDA4 and VCL-PEGDA8 phase transitions occurred broadly, showing LCST values of $(32.6 \pm 0.1)^\circ\text{C}$ and $(32.3 \pm 0.1)^\circ\text{C}$, respectively.

4.4 Particle Size Studies

The thermo-responsiveness studies demonstrated that VCL-PEGDA_x hydrogels show a phase transition when the temperature of the aqueous solution is above LCST ($\sim 32^\circ\text{C}$). Some studies showed that both hydrogen bond and hydrophobic interactions in the polymer-solvent system are the main responsible for phase transition above critical solution temperatures.[77] Thereby, PVCL-based hydrogels show a swollen state below critical solution temperature, in which the hydrogen bonding mainly governs the polymer confor-

mation. Upon temperature rises above the critical solution temperature, the hydrophobic interactions between polymer-polymer chains are favored, showing a collapsed state. [57] Table 4.4 and Table 4.5 show the mean particle size and polydispersity index (PDI) of VCL-PEGDA_x at temperatures below and above LCST, respectively. In general, a decrease in particle size for all VCL-PEGDA_x hydrogels is observed when the temperature rises above the previously determined LCST, which supports the phase transition from swollen to a collapsed state.

Table 4.4: Mean particle size and polydispersity index (PDI) of VCL-PEGDA_x at $T < LCST$.

	mean particle size (nm)	PDI
VCL-PEGDA0	31.8 ± 0.2	0.271 ± 0.011
VCL-PEGDA2	142.5 ± 13.7	0.386 ± 0.012
VCL-PEGDA4	1339.7 ± 73.9	0.299 ± 0.025
VCL-PEGDA8	361.9 ± 7.6	0.224 ± 0.039

Table 4.5: Mean particle size and polydispersity index (PDI) of VCL-PEGDA_x at $T > LCST$.

	mean particle size (nm)	PDI
VCL-PEGDA0	16.6 ± 1.9	0.005 ± 0.000
VCL-PEGDA2	8.3 ± 0.8	0.160 ± 0.029
VCL-PEGDA4	4.0 ± 0.3	0.194 ± 0.013
VCL-PEGDA8	2.3 ± 0.2	0.193 ± 0.002

Below LCST (Table 4.4), with the exception of VCL-PEGDA₄, the trend observed is the growth in the mean particle size of VCL-PEGDA_x when the PEGDA crosslinker content is increased. As mentioned in background information, PEGDA is a hydrophilic crosslinker. Thereby, the addition of PEGDA favors the hydrogen bonding between polymer and solvent, and this could explain the increment in the mean particle size at this condition. On the other hand, above LCST (Table 4.5), a phase transition occurs from swollen to collapsed state. This might be explained by the polymer-polymer interactions predominating over the polymer-solvent interactions at this state.[57] Although the mean particle size at this temperature does not show significant differences in order of magnitude, the observed trend is a decrease in mean particle size when the PEGDA amount increases.

It might be attributed also to the PEGDA contribution making that polymer-polymer interactions overcomes polymer-solvent interactions. Additionally, it has been demonstrated that PEGDA acts as a stabilizer.[73] Therefore, the presence of PEGDA, acting as a polymer surfactant, might contribute to the decrease in the mean particle size of VCL-PEGDA_x hydrogels.

4.5 Uptake and Release Studies

The potential application of poly(VCL-co-PEGDA) hydrogels as drug delivery carriers was investigated using colchicine as a model drug.

Drug loading was quantified by the HPLC analytical method described in Section 3.4.5 using the calibration curve of range 5-100 $\mu\text{g}/\text{mL}$. The parameters of the calibration curve obtained are summarized in Table 4.6, and calibration curve is given in Figure 4.7.

Table 4.6: Calibration curve parameters (5-100 $\mu\text{g}/\text{mL}$).

Parameters	Value
Concentration range of colchicine standards	5-100 $\mu\text{g}/\text{mL}$
Correlation coefficient	0.9991
Linearity Intercept	$(0.6 \pm 0.8) \text{ mAu} \cdot \text{min}$
Slope	$(0.94 \pm 0.01) \text{ mL} \cdot \text{mAu} \cdot \text{min}/\mu\text{g}$
Retention time	2.107 min

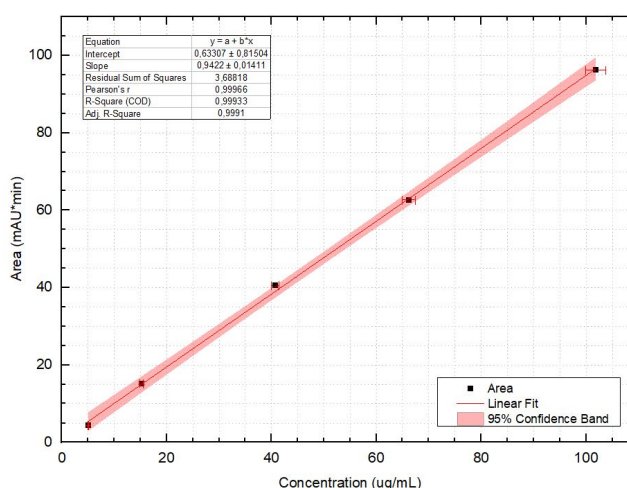


Figure 4.7: Calibration curve of colchicine (5-100 $\mu\text{g}/\text{mL}$).

Drug loading and encapsulation efficiency of VCL-PEGDA_x hydrogels are shown in Table 4.7. Drug loading (DL) is defined by the amount of drug-loaded per unit weight of the

hydrogel, while encapsulation efficiency (EE) is the actual drug amount in the hydrogel over the initial amount added. As can be observed, the drug loading did not change meaningfully by the crosslinker addition, ranging from $(1.1 \pm 0.2)\%$ to $(1.7 \pm 0.2)\%$. On the other hand, the encapsulation efficiency tends to decrease when the crosslinked amount increases.

Table 4.7: Drug Loading (% DL) and Encapsulation Efficiency (% EE) of VCL-PEGDAx hydrogels.

	DL (%)	EE (%)
VCL-PEGDA0	1.4 ± 0.2	37.5 ± 10.8
VCL-PEGDA2	1.7 ± 0.2	37.3 ± 10.9
VCL-PEGDA4	1.2 ± 0.2	35.0 ± 11.0
VCL-PEGDA8	1.1 ± 0.2	30.3 ± 11.4

On the other hand, drug release was quantified by the HPLC analytical method described in Section 3.4.5 using the calibration curve of range 2-20 $\mu\text{g}/\text{mL}$. The parameters of the calibration curve obtained are summarized in Table 4.8, and calibration curve is given in Figure 4.8.

Table 4.8: Calibration curve parameters (2-20 $\mu\text{g}/\text{mL}$).

Parameters	Value
Concentration range of colchicine standards	2-20 $\mu\text{g}/\text{mL}$
Correlation coefficient	0.99873
Linearity Intercept	$(-0.6 \pm 0.3) \text{ mAu} \cdot \text{min}$
Slope	$(1.06 \pm 0.02) \text{ mL} \cdot \text{mAu} \cdot \text{min}/\mu\text{g}$
Retention time	2.260 min

To understand the drug release from the colchicine-loaded VCL-PEGDAx hydrogels, the release profiles are shown in Figure 4.9. In general, a sustained release was obtained for all VCL-PEGDA hydrogels. The release profile observed in all hydrogels used in this study showed a gentle slope at the beginning followed by a plateau whose appearance and maximum value depends on the hydrogel composition.

Thus, the maximum % of cumulative release appear to be a function or crosslinker content in the hydrogel and follow this order: VCL-PEGDA8 > VCL-PEGDA4 > VCL-PEGDA2, corresponding to PEGDA crosslinker content of 8, 4 and 2 wt %, respectively. This trend also, as previously commented, can be associate to more collapse gel state and smaller gel average particle size with higher polymer PEGDA crosslinker content. VCL-PEGDA0

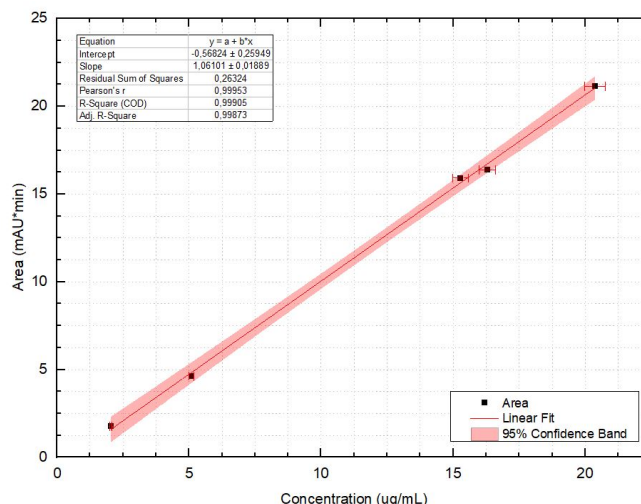


Figure 4.8: Calibration curve of colchicine (2-20 $\mu\text{g}/\text{mL}$).

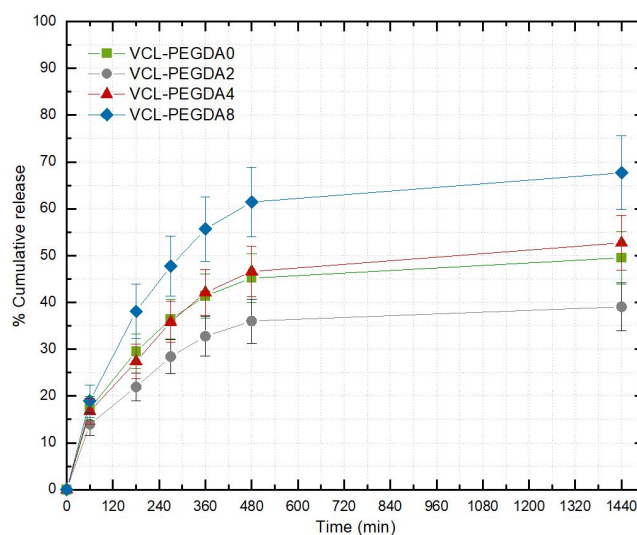


Figure 4.9: Cumulative release (%) of colchicine at $T = 38^\circ\text{C}$.

do not follow this trend and this can be explained by the fact that it is the homolymer PVCL synthesized without any crosslinker agent.

It has been stated that smart hydrogels have many advantages in the following situations:

(a) a sustained constant concentration of the drug in the body is desired, (b) the bio-active compound has a very short half-time, (c) the drug has strong side-effects or stability problems, (d) it is necessary to achieve a better patient compliance, and (e) the drug is wasted or taken in frequent dosage. [56] In this stage of the research, the design of the hydrogels prepared in this study fulfill the requirement of a sustained release of the colchicine as drug with low therapeutic index. [4] Similar drug release profiles has been observed for other PNVCL-based hydrogels.[59, 68, 77, 78]

This page is intentionally left blank.

Chapter 5

Conclusions and Recommendations

5.1 Conclusions

This work has led us to conclude that:

1. Four thermo-responsive polymeric hydrogels were synthesized through emulsion polymerization of N-vinyl caprolactam (VCL) crosslinked with different amounts of poly(ethylene glycol) diacrylate (PEGDA).
2. FTIR results confirmed the chemical structures of hydrogels PNVCL-based hydrogels crosslinked with PEGDA.
3. The cloud point of VCL-PEGDA_x hydrogels showed values near 32 °C, and confirms the synthesis of thermo-responsive hydrogels.
4. The phase transition, as shown by the cloud point values, is slightly affected by the crosslinker amount in the polymeric hydrogel.
5. For low crosslinker concentration, a sharp phase transition is observed, while a high content of PEGDA broad phase transition is shown.
6. Below LCST, the solvent-polymer interactions predominate and the hydrogels shows swollen nanostructures, as evidence of a trend in particle size growths when the of PEGDA content is increased in the polymer.
7. Above LCST, the polymer-polymer interactions predominate, so the hydrogels show collapsed states. Correspondingly, the hydrogel mean particle size tends to decrease when the PEGDA crosslinker content increases.
8. A sustained release was observed for all VCL-PEGDA_x hydrogels. The hydrogel containing a lower amount of PEGDA showed a better drug loading capacity, while the increment of PEGDA amounts showed a better release profile.
9. The maximum % of cumulative of colchicine release appear to be a function of crosslinker content in the hydrogel and follows the following order: VCL-PEGDA₈ > VCL-PEGDA₄ > VCL-PEGDA₂. This trend can be associate to more collapsed gel state and smaller gel mean particle size with higher PEGDA crosslinker content in the polymer.

10. Similar drug release profiles have been observed for other PNVCL based hydrogels reported in the literature.[59, 68, 77, 78]

5.2 Recommendations

It is recommended that further research should be undertaken in the following aspects:

1. To study in detail the influence of variables such as emulsifier and initiator concentration in order to determine their influence in the average particle size.
2. To use other state-of-the-art characterization techniques such as DSC, SEM, TEM, AFM, and NMR in order to have additional information on this polymeric hydrogel and their interaction with colchicine.
3. To use other techniques such as DSC and fully temperature controlled DLS to determine the LCST of polymeric hydrogels.
4. To extend this study to other drugs release mechanism (i.e., centrifugation), and for other type of therapeutic drugs.
5. To develop other types of smart polymeric hydrogels with the capability to react to stimuli such changes in pH values.

References

- (1) Zhang, Y.; Chan, H. F.; Leong, K. W. *Advanced Drug Delivery Reviews* **2013**, *65*, 104–120.
- (2) Zhang, J.; Misra, R. *Acta Biomaterialia* **2007**, *3*, 838–850.
- (3) Bai, J.; Wang, J. T.-W.; Rubio, N.; Protti, A.; Heidari, H.; Elgogary, R.; Southern, P.; Al-Jamal, W. T.; Sosabowski, J.; Shah, A. M.; Bals, S.; Pankhurst, Q. A.; Al-Jamal, K. T. *Theranostics* **2016**, *6*, 342–356.
- (4) Niel, E.; Scherrmann, J.-M. *Joint Bone Spine* **2006**, *73*, 672–678.
- (5) Langer, R. *Science* **1990**, *249*, 1527–1533.
- (6) Abu-Thabit, N. Y.; Makhoul, A. S. H. In *Stimuli Responsive Polymeric Nanocarriers for Drug Delivery Applications, Volume 1*, Makhoul, A. S. H., Abu-Thabit, N. Y., Eds.; Woodhead Publishing Series in Biomaterials; Woodhead Publishing: 2018, pp 3–41.
- (7) Uhrich, K. E.; Cannizzaro, S. M.; Langer, R. S.; Shakesheff, K. M. *Chemical Reviews* **1999**, *99*, 3181–3198.
- (8) Bruck, S. D. In *Controlled Drug Delivery: Volume 1 Basic Concepts*, Bruck, S. D., Ed.; CRC Press: 2019, pp 1–13.
- (9) Zhang, Y.; Zhang, N.; Song, H.; Li, H.; Wen, J.; Tan, X.; Zheng, W. *Drug delivery* **2019**, *26*, 70–77.
- (10) M. Abdulbaqi, I.; Darwis, Y.; Abou Assi, R.; Khan, N. *Drug Design, Development and Therapy* **2018**, *Volume 12*, 795–813.
- (11) Goldfinger SE *New England Journal of Medicine* **1972**, *287*, 1302.
- (12) Sur, S.; Rathore, A.; Dave, V.; Reddy, K. R.; Chouhan, R. S.; Sadhu, V. *Nano-Structures & Nano-Objects* **2019**, *20*, 100397.
- (13) Aguirre, G.; Villar-Alvarez, E.; González, A.; Ramos, J.; Taboada, P.; Forcada, J. *Journal of Polymer Science Part A: Polymer Chemistry* **2016**, *54*, 1694–1705.
- (14) Ramos, J.; Forcada, J.; Hidalgo-Alvarez, R. *Chemical Reviews* **2014**, *114*, 367–428.
- (15) Oh, J. K.; Lee, D. I.; Park, J. M. *Progress in Polymer Science* **2009**, *34*, 1261–1282.

-
- (16) Pikabea, A.; Ramos, J.; Forcada, J. *Particle & Particle Systems Characterization* **2014**, *31*, 101–109.
- (17) Osada, Y.; Kajiwara, K., *Gels Handbook, Four-Volume Set*; Gels handbook; Elsevier Science: 2000.
- (18) Ullah, F.; Othman, M. B. H.; Javed, F.; Ahmad, Z.; Akil, H. M. *Materials Science and Engineering: C* **2015**, *57*, 414–433.
- (19) Jiang, Y.; Chen, J.; Deng, C.; Suuronen, E. J.; Zhong, Z. *Biomaterials* **2014**, *35*, 4969–4985.
- (20) Soni, K. S.; Desale, S. S.; Bronich, T. K. *Journal of Controlled Release* **2016**, *240*, 109–126.
- (21) Ahmed, E. M. *Journal of Advanced Research* **2015**, *6*, 105–121.
- (22) Jagur-Grodzinski, J. *Polymers for Advanced Technologies* **2009**, *21*, 27–47.
- (23) Wack, H.; Ulbricht, M. *Industrial & Engineering Chemistry Research* **2006**, *46*, 359–364.
- (24) Dušek, K.; Patterson, D. *Journal of Polymer Science B Polymer Physics* **1968**, *6*, 1209–1216.
- (25) Kopecek, J. *Biomaterials* **2008**, *28*, 5185–92.
- (26) Maji, S.; Jerca, V. V.; Jerca, F. A.; Hoogenboom, R. In *Polymeric Gels*, Pal, K., Banerjee, I., Eds.; Woodhead Publishing Series in Biomaterials; Woodhead Publishing: 2018, pp 3–27.
- (27) Gutowska, A.; Bae, Y.; Feijen, J.; Kim, S. *Journal of Controlled Release* **1992**, *22*, 95–104.
- (28) Sun, F.; Wang, Y.; Wei, Y.; Cheng, G.; Ma, G. *Journal of Bioactive and Compatible Polymers* **2014**, *29*, 301–317.
- (29) Ter Schiphorst, J.; Coleman, S.; Stumpel, J. E.; Ben Azouz, A.; Diamond, D.; Schenning, A. P. H. J. *Chemistry of Materials* **2015**, *27*, 5925–5931.
- (30) Tomatsu, I.; Peng, K.; Kros, A. *Advanced Drug Delivery Reviews* **2011**, *63*, 1257–1266.
- (31) D’Emanuele, A.; Staniforth, J. N. *Pharmaceutical Research* **1991**, *8*, 913–918.

- (32) Agnihotri, S.; Kulkarni, R.; Nadagouda, M.; Kulkarni, P.; Aminabhavi, T. *Journal of Applied Polymer Science* **2005**, *96*, 301–311.
- (33) Creque, H. M.; Langer, R.; Folkman, J. *Diabetes* **1980**, *29*, 37–40.
- (34) Muzzalupo, R.; Tavano, L.; Oliviero, C.; Picci, N.; Ranieri, G. *Colloids and surfaces. B, Biointerfaces* **2015**, *134*, 273–278.
- (35) Patel, V. R.; Amiji, M. M. *Pharmaceutical Research* **1996**, *13*, 588–593.
- (36) Jianqi, F.; Lixia, G. *European Polymer Journal* **2002**, *38*, 1653–1658.
- (37) Park, T. G.; Hoffman, A. S. *Macromolecules* **1993**, *26*, 5045–5048.
- (38) Kumar, A.; Galaev, I. Y.; Mattiasson, B. *Biotechnology and Bioengineering* **1998**, *59*, 695–704.
- (39) Brown, L. R.; Edelman, E. R.; Fischel-Ghodsian, F.; Langer, R. *Journal of Pharmaceutical Sciences* **1996**, *85*, 1341–1345.
- (40) Kang, S. I.; Bae, Y. H. *Journal of Controlled Release* **2003**, *86*, 115–121.
- (41) Kim, H. K.; Shim, W. S.; Kim, S. E.; Lee, K.-H.; Kang, E.; Kim, J.-H.; Kim, K.; Kwon, I. C.; Lee, D. S. *Tissue Engineering Part A* **2009**, *15*, 923–933.
- (42) Chatterjee, S.; Hui, P. C.-l.; Kan, C.-w.; Wang, W. *Scientific Reports* **2019**, *9*, 11658.
- (43) Miyata, T.; Asami, N.; Uragami, T. *Nature* **1999**, *399*, 766–769.
- (44) Suzuki, Y.; Tanihara, M.; Nishimura, Y.; Suzuki, K.; Kakimaru, Y.; Shimizu, Y. *Journal of Biomedical Materials Research* **1998**, *42*, 112–116.
- (45) Lau, A. C. W.; Wu, C. *Macromolecules* **1999**, *32*, 581–584.
- (46) Hoare, T. R.; Kohane, D. S. *Polymer* **2008**, *49*, 1993–2007.
- (47) Wang, Y.; Nie, J.; Chang, B.; Sun, Y.; Yang, W. *Biomacromolecules* **2013**, *14*, 3034–3046.
- (48) Galperin, A.; Long, T.; Ratner, B. *Biomacromolecules* **2010**, *11*, 2583–92.
- (49) Kowalczyk, A.; Fau, M.; Karbarz, M.; Donten, M.; Stojek, Z.; Nowicka, A. *Biosensors & bioelectronics* **2013**, *54C*, 222–228.
- (50) He, L.; Fullenkamp, D.; Rivera, J.; Messersmith, P. *Chemical communications (Cambridge, England)* **2011**, *47*, 7497–9.

- (51) Lee, B. P.; Konst, S. *Advanced Materials* **2014**, *26*, 3415–3419.
- (52) Lee, P. I.; Li, J.-X. In *Oral Controlled Release Formulation Design and Drug Delivery*; John Wiley & Sons, Ltd: 2010; Chapter 2, pp 21–31.
- (53) Kreuter, J. *International journal of pharmaceutics* **2007**, *331*, 1–10.
- (54) Rao, K.; Rao, K.; Ha, C.-S. *Gels* **2016**, *2*, 6.
- (55) Gupta, P.; Vermani, K.; Garg, S. *Drug Discovery Today* **2002**, *7*, 569–579.
- (56) Bajpai, A. K.; Shukla, S. K.; Bhanu, S.; Kankane, S. *Progress in Polymer Science* **2008**, *33*, 1088–1118.
- (57) Teotia, A.; Sami, H.; Kumar, A. In *Switchable and Responsive Surfaces and Materials for Biomedical Applications*, Zhang, Z., Ed.; Woodhead Publishing: Oxford, 2015, pp 3–43.
- (58) Alsuraifi, A.; Curtis, A.; Lamprou, D. A.; Hoskins, C. *Pharmaceutics* **2018**, *10*, 136.
- (59) Vihola, H.; Laukkanen, A.; Tenhu, H.; Hirvonen, J. *Journal of Pharmaceutical Sciences* **2008**, *97*, 4783–4793.
- (60) Shin, J.; Braun, P. V.; Lee, W. *Sensors and Actuators B: Chemical* **2010**, *150*, 183–190.
- (61) Bordat, A.; Boissenot, T.; Nicolas, J.; Tsapis, N. *Advanced Drug Delivery Reviews* **2019**, *138*, 167–192.
- (62) Mohammed, M. N.; Yusoh, K. B.; Shariffuddin, J. H. B. H. *Materials Express* **2018**, *8*, 21–34.
- (63) Imaz, A.; Forcada, J. *Journal of Polymer Science Part A: Polymer Chemistry* **2008**, *46*, 2510–2524.
- (64) Vihola, H.; Laukkanen, A.; Valtola, L.; Tenhu, H.; Hirvonen, J. *Biomaterials* **2005**, *26*, 3055–3064.
- (65) Sun, S.; Wu, P. *The Journal of Physical Chemistry B* **2011**, *115*, 11609–11618.
- (66) Dalton, M.; Halligan, S.; Killion, J.; Murray, K.; Geever, L. *Advances in Environmental Biology* **2014**, *8*, 1–6.

- (67) Cortez-Lemus, N. A.; Licea-Claverie, A. *Progress in Polymer Science* **2016**, *53*, 1–51.
- (68) Rao, K. M.; Mallikarjuna, B.; Rao, K. K.; Siraj, S.; Rao, K. C.; Subha, M. *Colloids and Surfaces B: Biointerfaces* **2013**, *102*, 891–897.
- (69) Maudens, P.; Meyer, S.; Seemayer, C. A.; Jordan, O.; Allémann, E. *Nanoscale* **2018**, *10*, 1845–1854.
- (70) Panja, S.; Dey, G.; Bharti, R.; Kumari, K.; Maiti, T. K.; Mandal, M.; Chattopadhyay, S. *ACS Applied Materials & Interfaces* **2016**, *8*, 12063–12074.
- (71) Sudhakar, K.; Rao, K. M.; Subha, M. C. S.; Rao, K. C.; Sadiku, E. R. *Designed Monomers and Polymers* **2015**, *18*, 705–713.
- (72) Son, K. H.; Lee, J. W. *Materials* **2016**, *9*, 854.
- (73) Imaz, A.; Forcada, J. *Journal of Polymer Science Part A: Polymer Chemistry* **2008**, *46*, 2766–2775.
- (74) Gowda, B. *International Journal of Pharmacy and Pharmaceutical Sciences* **2014**, *6*, 335–337.
- (75) Gola, A.; Nizniowska, A.; Musiał, W. *Nanomaterials (Basel, Switzerland)* **2019**, *9*, 1577.
- (76) Liu, F.; Kozlovskaya, V.; Kharlampieva, E. **2018**, 93–120.
- (77) Wang, Y.; Nie, J.; Chang, B.; Sun, Y.; Yang, W. *Biomacromolecules* **2013**, *14*, 3034–3046.
- (78) Madhusudana Rao, K.; Krishna Rao, K. S.; Sudhakar, P.; Chowdoji Rao, K.; Subha, M. C. *Journal of Applied Pharmaceutical Science* **2013**, *3*, 61–69.

This page is intentionally left blank.

Attachments

A. Inform of DLS results.



ESCUELA POLITÉCNICA NACIONAL LABORATORIO DE NUEVOS MATERIALES (LANUM)

Campus Politécnico "José Rubén Orellana Ricaurte" • Calle Isabela Católica S/N y Alfredo Mena Caamaño
RUC: 1760005620001 • Tel.: (00593-2) 2976300 Ext.: 3000, 3002, 3735
Apartado 17-01-2759 • E-mail: lanum.fim@epn.edu.ec • Quito – Ecuador



INFORME DE RESULTADOS No. II-2020-004

Solicitud de trabajo No. LANUM-2020-ST.006

Quito, 28 de enero de 2020

DATOS DE LA EMPRESA/INSTITUCIÓN SOLICITANTE

Solicitado por: Dr. Antonio Díaz
Empresa / Institución: Universidad Yachay Tech (Investigador)
Teléfono: +593 98 0900 506
Dirección: San Miguel de Urququí, Hacienda San José s/n
E-Mail: adiaz@yachaytech.edu.ec
Identificación de la(s) muestra(s) (cliente):

002GD
003GD
004GD
005GD
T002GD

Descripción de la(s) muestra(s): Suspensiones acuosas

LABORATORIO

Fecha de ingreso al Laboratorio: 22/01/2020
Identificación de la(s) muestra(s) (código LANUM):

- MI-20-0102 (002GD)
- MI-20-0103 (003GD)
- MI-20-0104 (004GD)
- MI-20-0105 (005GD)
- MI-20-0106 (T002GD)

Fecha en que se realizó el ensayo: 22/01/2020
Área del laboratorio donde se realizó el ensayo: Área de análisis

Condiciones ambientales

Temperatura: 22,1°C Humedad: 50,1 % HR

EQUIPOS UTILIZADOS

- Analizador de tamaño de partícula y potencial Z, Marca Brookhaven, Modelo 90 Plus.

MÉTODO EMPLEADO

- Medición del tamaño de partícula de suspensiones acuosas (procedimiento propio del laboratorio). Las condiciones del ensayo se detallan a continuación:
Número de corridas: 5

NPR

F-PT-07-05

Página 1 de 5



ESCUELA POLITÉCNICA NACIONAL LABORATORIO DE NUEVOS MATERIALES (LANUM)

Campus Politécnico "José Rubén Orellana Ricaurte" • Calle Isabela Católica S/N y Alfredo Mena Caamaño
RUC: 1760005620001 • Tel.: (00593-2) 2976300 Ext.: 3000, 3002, 3735
Apartado 17-01-2759 • E-mail: lanum.fim@epn.edu.ec • Quito – Ecuador



RESULTADOS

A continuación, se presentan los resultados de los análisis de tamaño de partícula.

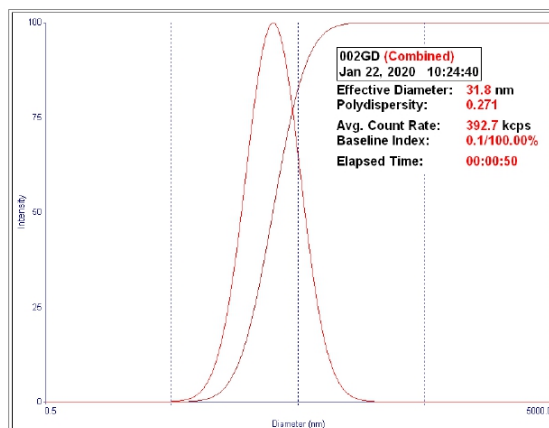


Figura 1. Tamaño de partícula de la muestra 002GD (MI-20-0102)

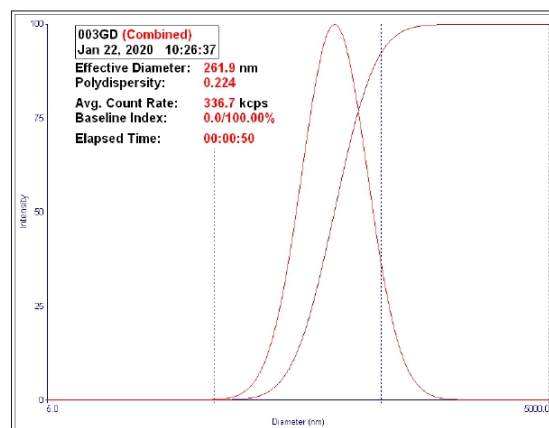


Figura 2. Tamaño de partícula de la muestra 003GD (MI-20-0103)



ESCUELA POLITÉCNICA NACIONAL
LABORATORIO DE NUEVOS MATERIALES (LANUM)

Campus Politécnico "José Rubén Orellana Ricaurte" • Calle Isabela Católica S/N y Alfredo Mena Caamaño
 RUC: 1760005620001 • Tel.: (00593-2) 2976300 Ext.: 3000, 3002, 3735
 Apartado 17-01-2759 • E-mail: lanum.fim@epn.edu.ec • Quito – Ecuador

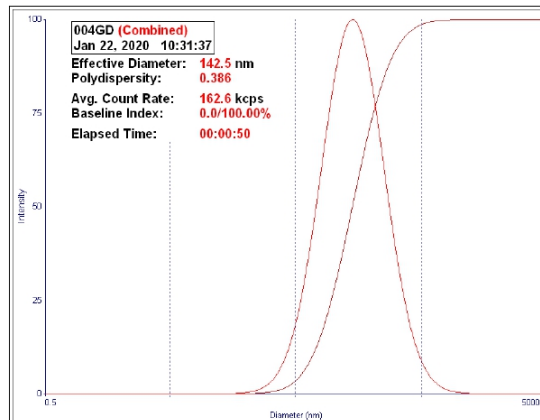


Figura 3. Tamaño de partícula de la muestra 004GD (MI-20-0104)

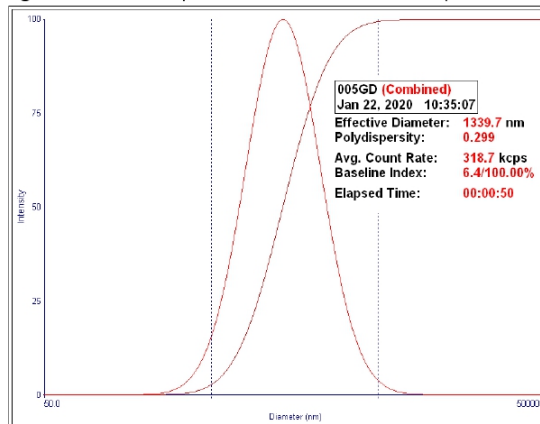


Figura 4. Tamaño de partícula de la muestra 005GD (MI-20-0105)

NPR



ESCUELA POLITÉCNICA NACIONAL
LABORATORIO DE NUEVOS MATERIALES (LANUM)

Campus Politécnico "José Rubén Orellana Ricaurte" • Calle Isabela Católica S/N y Alfredo Mena Caamaño
 RUC: 1760005620001 • Tel.: (00593-2) 2976300 Ext.: 3000, 3002, 3735
 Apartado 17-01-2759 • E-mail: lanum.fim@epn.edu.ec • Quito – Ecuador

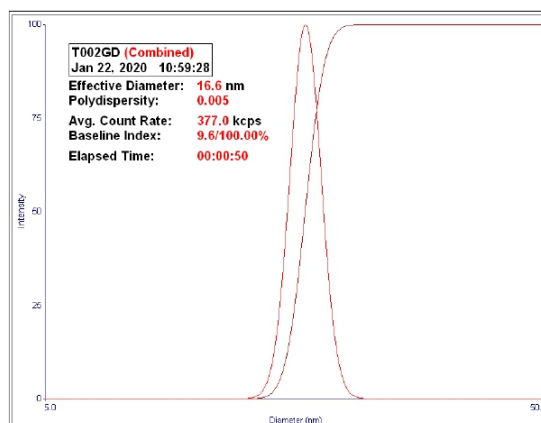


Figura 5. Tamaño de partícula de la muestra T002GD (MI-20-0106)

Cabe indicar que el diámetro efectivo corresponde a un promedio global del tamaño de las partículas en suspensión. Los valores promedio del tamaño de partícula de las muestras se detallan en la tabla 1.

Tabla 1. Tamaño de partícula de las muestras

Nombre de la muestra	Diámetro efectivo promedio (nm)	Polidispersidad
002GD (MI-20-0102)	31,8	0,271
003GD (MI-20-0103)	261,9	0,224
004GD (MI-20-0104)	142,5	0,386
005GD (MI-20-0105)	1339,7	0,299
T002GD (MI-20-0106)	16,6	0,005

El cliente puede hacer uso académico de los resultados presentados en este informe, así como de los respaldos enviados en formato electrónico para su tratamiento.

OBSERVACIÓN: La normativa para la organización y gestión de los laboratorios de la Escuela Politécnica Nacional, capítulo IV (De la difusión) menciona: "Si la contribución de un laboratorio es significativa y sustancial para la realización de una publicación, se deberá colocar al miembro(s) del laboratorio que contribuyó al desarrollo de la investigación como co-autor(es) de la publicación realizada". En este caso, por favor mantener comunicado al LANUM.

MPR



ESCUELA POLITÉCNICA NACIONAL
LABORATORIO DE NUEVOS MATERIALES (LANUM)

Campus Politécnico "José Rubén Orellana Ricaurte" • Calle Isabela Católica S/N y Alfredo Mena Caamaño
RUC: 1760005620001 • Tel.: (00593-2) 2976300 Ext.: 3000, 3002, 3735
Apartado 17-01-2759 • E-mail: lanum.fim@epn.edu.ec • Quito – Ecuador



**NOTA: ESTOS RESULTADOS ESTÁN RELACIONADOS ÚNICAMENTE A LA(S) MUESTRA(S)
SOMETIDA(S) A ENSAYO**

Realizado por:

Ing. Salomé Galeas H.
Analista Técnica

Revisado y aprobado por:

Ing. Orlando Campaña
Responsable Técnico (S)

Autorizado por:

Paulina Romero, Ph.D.
Coordinadora del Laboratorio

B. Calculations of Total Solids.

instrument errors	
micropipette (mL)	0.018
analytical balance (mg)	0.0005

n	3
---	---

VCL-PEGDA0

#	Petri dish	initial gel	Petri dish+gel	w/v	w/v average		conc. gel	
	(g)	(mL)	(g)	%	%	err	mg/mL	err
1	37,306	2.0	37,336	1,50	1,50	0,02	14,98	0,23
2	36,943	0,5	36,951	1,52				
3	37,587	2.0	37,617	1,47				

VCL-PEGDA2

#	Petri dish	initial gel	Petri dish+gel	w/v	w/v average		conc. gel	
	(g)	(mL)	(g)	%	%	err	mg/mL	err
1	46,193	2.0	46,218	1,23	1,24	0,01	12,37	0,08
2	37,306	2.0	37,331	1,23				
3	37,347	2.0	37,372	1,24				

VCL-PEGDA4

#	Petri dish	initial gel	Petri dish+gel	w/v	w/v average		conc. gel	
	(g)	(mL)	(g)	%	%	err	mg/mL	err
1	37,323	2.0	37,355	1,59	1,65	0,05	16,52	0,54
2	44,237	2.0	44,270	1,67				
3	46,167	2.0	46,201	1,69				

VCL-PEGDA8

#	Petri dish	initial gel	Petri dish+gel	w/v	w/v average		conc. gel	
	(g)	(mL)	(g)	%	%	err	mg/mL	err
1	37,346	2.0	37,376	1,50	1,50	0,01	14,95	0,13
2	44,265	2.0	44,295	1,48				
3	46,193	0,5	46,200	1,50				

C. Calculations of yields.

	VCL-PEGDA0	VCL-PEGDA2	VCL-PEGDA4	VCL-PEGDA8
water 1 (mg)	276.20	270.72	276.50	270.13
SDS (mg)	0.1016	0.1063	0.1058	0.1042
VCL (mg)	5.7617	6.0186	6.0028	6.0089
PEGDA (mg)	0.0000	0.1314	0.2404	0.4926
NAHCO3 (mg)	0.0369	0.1012	0.1004	0.1031
APS (mg)	0.0309	0.0444	0.041	0.0404
water 2 (mg)	8.06	18.30	18.20	18.03

intrument errors	
analytical balance (mg)	5E-04
balance (mg)	0.05

total mass (mg)	290.194	295.422	301.190	294.914
M1 (mg)	5.931	6.402	6.490	6.749
M2 (mg)	284.263	289.020	294.700	288.165
TS theor. (%w/v)	2.086	2.215	2.202	2.342
err(TS theor.)	0.001	0.001	0.001	0.001

err(M1)	0.0011
err(M2)	0.0707

TS exp. (%w/v)	1.50	1.24	1.65	1.50
err(TS exp.)	0.02	0.01	0.05	0.01

% yield	71.8	55.8	75.0	63.8
err(yield)	1.1	0.3	2.4	0.6

D. Calculations of standard solutions.

COLCHICINE STOCK	
conc. (mg/mL)	1
vol. (mL)	25
purity	0.95
theoretical mass	26,32

ERRORS		
experimental mass	26,8	mg
volumen	25	mL
err(analytical balance)	0,5	mg
err(volumetric25ml)	0,04	mL
conc stock	1018,40	ug/mL
err(conc stock)	19,07	ug/mL
err(micropipette)	0,0006	mL
err(volumetric10ml)	0,0250	mL

	STD2	STD5	STD15	STD16	STD20	STD40	STD65	STD100
conc. (mg/mL)	2	5	15	16	20	40	65	100
vol. (mL)	10							
from theor. conc. stock (ug/mL)	1000,00							
V1 stock (mL)	0.020	0,050	0,150	0,160	0,200	0,400	0,650	1,000
V1 stock (uL)	20,0	50,0	150,0	160,0	200,0	400,0	650,0	1000,0
C2 (ug/mL)	2,04	5,09	15,28	16,29	20,37	40,74	66,20	101,84
err(C2)	0,07	0,11	0,29	0,31	0,39	0,77	1,25	1,92

E. Calibration curve data (5-100 $\mu\text{g}/\text{mL}$).

	Concentration		Area	n	5
	ug/mL	err	mAU*min		
STD	5.1	0.1	4.4	SLOPE	0,94
	15,3	0.3	15,2	INTERCEPT	0,63
	40.7	0.8	40.6	* SE reg	1,109
	66.2	1.3	62.7	Mean of Y	43,81
	101.8	1.9	96.2	Variance, of X	1542,74
			t(n-2,95%)	3,18	

		Area	Conc		
		mAU*min	ug/mL	(uncertainty)	err
VCL-PEGDA0	MC6_0	86,3	90,9	1,5	4,7
VCL-PEGDA2	MC8_0	86,6	91,3	1,5	4,8
VCL-PEGDA4	MC5_0	89,7	94,6	1,5	4,8
VCL-PEGDA8	MC7_0	96,2	101,5	1,6	5,0

F. Calculations of Drug Release (DL) and Encapsulation Efficiency (EE).

COLCHICINE STOCK			
	error		
real conc.	1018,4	19,1	ug/mL
volumen taken (micropipette)	5,0000	0,0006	mL
mass added	5092,0	95,4	ug
volumen (grad. cilinder)	35,0	0,5	mL
initial conc.	145,5	3,4	ug/mL

HYDROGEL STOCK				
	V gel		TS_exp	
	mL	err	mg/ml	err
VCL-PEGDA0			14,98	0,23
VCL-PEGDA2			12,37	0,08
VCL-PEGDA4			16,52	0,54
VCL-PEGDA8	9,00	0,04	14,95	0,13

	Conc. (not encap)		Conc. (encap)		encap amount		gel amount		D.L.		E.E.	
	ug/mL	err	ug/mL	err	ug	err	ug	err	%	err	%	err
VCL-PEGDA0	90,9	4,7	54,6	5,9	1911,0	206,6	134850,0	2097,2	1,4	0,2	37,5	4,1
VCL-PEGDA2	91,3	4,8	54,2	5,9	1897,5	206,9	111300,0	814,7	1,7	0,2	37,3	4,1
VCL-PEGDA4	94,6	4,8	50,9	5,9	1782,4	209,1	148650,0	4888,6	1,2	0,2	35,0	4,2
VCL-PEGDA8	101,5	5,0	44,0	6,1	1540,4	214,3	134550,0	1302,6	1,1	0,2	30,3	4,2

G. Calibration curve data (2-20 $\mu\text{g}/\text{mL}$).

	Concentration		Area
	ug/mL	err	mAU*min
STD	2.0	0.1	1.8
	5.1	0.1	4.6
	15.3	0.3	15.9
	16.3	0.3	16.4
	20.4	0.4	21.1

n	5
SLOPE	1.06
INTERCEPT	-0.57
* SE reg	0.296
Mean of Y	11.97
Variance, of X	61.50
t(n-2,95%)	3.18

		Area	Conc		
		mAU*min	ug/mL	(uncertainty)	err
VCL-PEGDA0	MC6_1	16.5	16.1	0.3	1.0
	MC6_2	3.4	3.7	0.3	1.1
	MC6_3	2.3	2.7	0.3	1.1
	MC6_4	1.6	2.1	0.4	1.1
	MC6_5	1.9	2.4	0.3	1.1
	MC6_6	9.5	9.5	0.3	1.0

VCL-PEGDA2	MC8_1	12.0	11.9	0.3	1.0
	MC8_2	3.2	3.5	0.3	1.1
	MC8_3	1.9	2.4	0.3	1.1
	MC8_4	1.3	1.8	0.4	1.1
	MC8_5	1.2	1.7	0.4	1.1
	MC8_6	7.5	7.6	0.3	1.0

VCL-PEGDA4	MC5_1	14.2	13.9	0.3	1.0
	MC5_2	4.0	4.3	0.3	1.1
	MC5_3	2.8	3.2	0.3	1.1
	MC5_4	1.9	2.3	0.3	1.1
	MC5_5	2.7	3.1	0.3	1.1
	MC5_6	8.5	8.5	0.3	1.0

VCL-PEGDA8	MC7_1	17.2	16.8	0.3	1.0
	MC7_2	3.9	4.2	0.3	1.1
	MC7_3	3.1	3.5	0.3	1.1
	MC7_4	2.1	2.5	0.3	1.1
	MC7_5	2.4	2.8	0.3	1.1
	MC7_6	8.3	8.3	0.3	1.0

H. Calculations of drug release.

VCL-PEGDA0

TIME		Conc. Release		% release		% acumulative	
h	min	ug/mL	err	ug/mL	err	%	err
0	0	0.0	0.0	0.0	0.0	0.0	0.0
1	60	9.5	1.0	17.3	2.6	17.3	2.6
3	180	16.1	1.0	29.5	3.7	29.5	3.7
4.5	270	3.7	1.1	6.9	2.1	36.4	4.2
6	360	2.7	1.1	5.0	2.1	41.4	4.7
8	480	2.1	1.1	3.8	2.1	45.2	5.2
24	1440	2.4	1.1	4.3	2.1	49.5	5.6

VCL-PEGDA2

TIME		Conc		% release		% acumulative	
h	min	ug/mL	err	ug/mL	err	%	err
0	0	0.0	0.0	0.0	0.0	0.0	0.0
1	60	7.6	1.0	14.0	2.4	14.0	2.4
3	180	11.9	1.0	21.9	3.0	21.9	3.0
4.5	270	3.5	1.1	6.5	2.1	28.4	3.6
6	360	2.4	1.1	4.3	2.1	32.8	4.2
8	480	1.8	1.1	3.3	2.1	36.0	4.7
24	1440	1.7	1.1	3.1	2.1	39.1	5.2

VCL-PEGDA4

TIME		Conc		% release		% acumulative	
h	min	ug/mL	err	ug/mL	err	%	err
0	0	0.0	0.0	0.0	0.0	0.0	0.0
1	60	8.5	1.0	16.7	2.8	16.7	2.8
3	180	13.9	1.0	27.4	3.7	27.4	3.7
4.5	270	4.3	1.1	8.5	2.3	35.8	4.4
6	360	3.2	1.1	6.3	2.3	42.1	4.9
8	480	2.3	1.1	4.5	2.2	46.6	5.4
24	1440	3.1	1.1	6.1	2.3	52.7	5.9

VCL-PEGDA8

TIME		Conc		% release		% acumulative	
h	min	ug/mL	err	ug/mL	err	%	err
0	0	0.0	0.0	0.0	0.0	0.0	0.0
1	60	8.3	1.0	18.9	3.5	18.9	3.5
3	180	16.8	1.0	38.1	5.8	38.1	5.8
4.5	270	4.2	1.1	9.6	2.8	47.7	6.4
6	360	3.5	1.1	7.9	2.7	55.7	6.9
8	480	2.5	1.1	5.8	2.6	61.4	7.4
24	1440	2.8	1.1	6.3	2.6	67.7	7.9